A PROPOSED GEOINDEX MODEL FOR DESIGN SELECTION OF NON-LINEAR PROPERTIES FOR SITE RESPONSE ANALYSES

Cliff Roblee and Brian Chiou
Caltrans Geo-Research Group
5900 Folsom Blvd., Sacramento, CA 95819

ABSTRACT

Laboratory test data on 154 natural soil samples obtained from 28 sites are used to develop a simple "GeoIndex Model" for design selection of dynamic soil properties for earthquake site response analyses. The GeoIndex model is parameterized similar to an earlier model proposed by Darendelli in 2001 [1, 2], with several adaptations made to accommodate the sensibilities of routine practice. The laboratory test data were developed using unique testing capabilities at the University of Texas (UT) and at the University of California Los Angeles (UCLA). The UT data were developed using a "resonant-column/torsional shear (RCTS)" device configured for application to very high pressures. The UCLA data were developed using "dual-specimen direct simple shear (DSDSS)" device capable of testing over a very wide strain range of interest to design applications. Two issues are examined using subsets of the overall data set. The first issue is an examination of systematic differences between laboratory results measured with different testing equipment and testing modes. A subset of 28 RCTS tests are used to compare resonant column and torsional shear results on identical specimens, and a subset of 9 "companion samples" were tested in both the RCTS and DSDSS equipment and are used to establish systematic trends between these test devices. The second issue is an examination of the effect of confining stress on measured properties. Average results for a subset of 26 RCTS tests are used to illustrate systematic trends, and a 1-to-1 relationship is proposed between the normalized modulus curve fit parameters and the low-strain velocity ratio.

The "GeoIndex model" is developed through a combination of statistical analyses and reasoned judgment, and ultimately presented as a tabulated set of equation coefficients and tabulated strain-dependent modulus reduction and damping curves, one set for each of 3 broad soil categories and 6 depth intervals. Predicted values of dynamic properties are plotted relative to all laboratory test results for each depth and soil-type bin, and statistics are developed to characterize data-model misfit. Comparisons are made with alternative depth-dependent and depth-independent models used in practice since the 1990's. Results for this experimental data set show significant bias at depth for the depth-independent models, and recommendations regarding the applicable depth range for each model are presented. Comparison of the simpler GeoIndex model with the more sophisticated Darendelli 2001 model show comparable levels of misfit for the data set considered.

1. INTRODUCTION

Earthquake site response analyses are often performed in geotechnical engineering practice to estimate non-linear amplification of earthquake ground motion caused by site-specific near-surface sediments. Basic parameters required for such an analysis include the shear-wave velocity profile and the non-linear stress-strain properties, or "dynamic properties", of the underlying sediments. The most common models for dynamic properties involve families of two strain-dependent parameters: modulus reduction (G/G_{max}) and hysteretic damping (D) that are typically presented as curves on a semi-log plot. While reasonably cost-effective techniques exist for site-specific measurement of local shear-wave profile, the high cost of sophisticated laboratory tests used to establish dynamic properties is typically prohibitive except for the most significant of projects. Therefore, practitioners typically make use of published values for dynamic properties where the assignment is based on a variety of geotechnical index parameters.

This paper proposes a simple new model for design selection of dynamic properties called the "GeoIndex model". The GeoIndex model is developed from recent high-quality data and incorporates key features of many predecessor models while accommodating the sensibilities of routine practice. Table 1

sketches the recent history of dynamic properties model development over the past couple decades, and provides insight into the basis for the GeoIndex model. Seed et.al. [3] provide a well established benchmark for dynamic properties of sandy soils. This model was based on numerous early laboratory results, primarily for confining pressures corresponding to the upper 10 meters of a soil column. Vucetic and Dobry [4] significantly extended knowledge of properties for clays, and developed a suite of six depth-independent design curves for different ranges of plasticity index (PI). Vucetic and Dobry's work was again based on testing at relatively low confining pressures. Idriss and Sun [5] included a pair of default depth-independent curves in SHAKE91, one for "sand" and another for "clay". Pyke [6] developed a set of depth-dependent curves known as the "EPRI curves" based on a combination of theory, literature findings and an extensive new testing program by Stokoe [7] on natural samples obtained over a wide range of depths from three ground-motion recording sites. The EPRI curves do not distinguish between soil types, but do show significant depth dependence with deeper deposits exhibiting more linear behavior. Silva et.al. [8] used seismological techniques in a comprehensive examination of source-path-site ground-motion modeling for multiple earthquakes under a project for the Brookhaven National Laboratories. This study deduced a set of dynamic properties known as the "BNL curves" that were considered the minimum soil non-linearity required to account for existing ground-motion observations. The BNL curves are an adaptation of the EPRI curves with a reduction in the number of curves from six to two, and a very significant shift toward more linear behavior at any given depth. Following the 1994 Northridge earthquake, an extensive series of new site investigations were performed at California strong-motion recording sites under the auspices of the ROSRINE projects and later extensions through the PEER-LL program, and through the "Near-Field Earthquake (NFE)" project performed in the US by Kajima Corporation of Japan. A significant contribution of these series of post-Northridge investigations has been to significantly extend the database of laboratory measured material properties for natural soils, with special emphasis on extending the range of confining pressure (UT tests) and range of strain (UCLA tests). Darendelli and Stokoe [1, 2] used initial results from these testing programs, plus an extensive proprietary database of additional test results, to develop an integrated model for dynamic properties that accommodates both depth dependence and differences in soil type. In that model, depth dependence is treated as a continuous function of effective confining stress, and soil type variations are treated as a continuous function of plasticity index (PI) and overconsolidation ratio (OCR). The model captures essential elements of earlier work including Seed et.al. sand, Vucetic and Dobry clays and provides depth dependence similar to that found in the EPRI curves.

Table 1 – Prediction Parameters for the GeoIndex Model and Alternative Models Used In Practice

Model	GeoIndex 2004	Darendelli & Stokoe 2001	BNL Silva et.al. 1997	EPRI Pyke 1993	SHAKE91 Idriss & Sun	Vucetic & Dobry 1991	Seed et.al. 1986

Prediction Basis
    Confinement:
    Soil Type:
	Yes
	Yes
		Yes
		Yes
			Yes
			No
				Yes
				No
					No
					Yes
						No
						Yes
							No
							Yes

Model for Soil Type	3 Discrete Groups = f(PI, P200)	Continuous Function = f(PI, OCR)	na	na	2 Discrete Groups: Sand, Clay	6 Discrete Groups = f(PI)	Range for Sands
Model for Confinement	6 Discrete Depth Bins	Continuous Function of Eff. Stress	2 Discrete Depth Bins	6 Discrete Depth Bins	na	na	na

The GeoIndex model proposed here draws extensively from the Darendelli 2001 model formulation, and can be considered an adaptation thereof that aims to incorporate the simplicity of many previous models and stresses ease of implementation for routine practice. While simple to apply, the GeoIndex model does retain essential features to allow for both depth and soil-type dependence. Primary modifications from the Darendelli [2001] model include:

1) Regressing modulus and damping curve coefficients directly for discrete depth and soil-type bins rather than establishing a unified functional form for simultaneous regression of the complete model;
2) Using three discrete soil groups based on PI and grain size (P200), rather than as a continuous function of PI and OCR, to account for the variation in properties with soil type;
3) Using six discrete soil depth ranges, rather than a continuous function of confining stress, to account for the variation in properties with depth;
4) Ignoring the effects of frequency and number of cycles on damping;
5) Allowing the shape of the modulus reduction curve (alpha coefficient described in Section 4) to differ for each of the 3 different soil types rather than fixing it to be constant for all soils.

The motivation for pursuing this investigation is twofold: 1) to provide an independent examination of recent laboratory data that will allow epistemic (i.e. modeling) uncertainty to be characterized, and 2) facilitation of implementation through development of a simple model form that can be readily applied in practice. On the second point, the GeoIndex model form requires that one of three easily defined soil types be specified for any given depth range. The soil types are defined broadly so that specification can be applied to stratigraphic layers classified on the basis of simple index tests (PI and P200) or estimated based on visual classification. As illustrated in Fig. 1, real soil profiles often involve significant variations in index tests such as PI within any given strata, and specification of different curve sets for such variations could lead to an impractical level of detail in a site response calculation that misses the overall level of uncertainty inherent to ground-motion prediction. While it is recognized that model simplifications can increase prediction error, Section 8 illustrates that the penalty for adopting the simpler model form is quite acceptable.
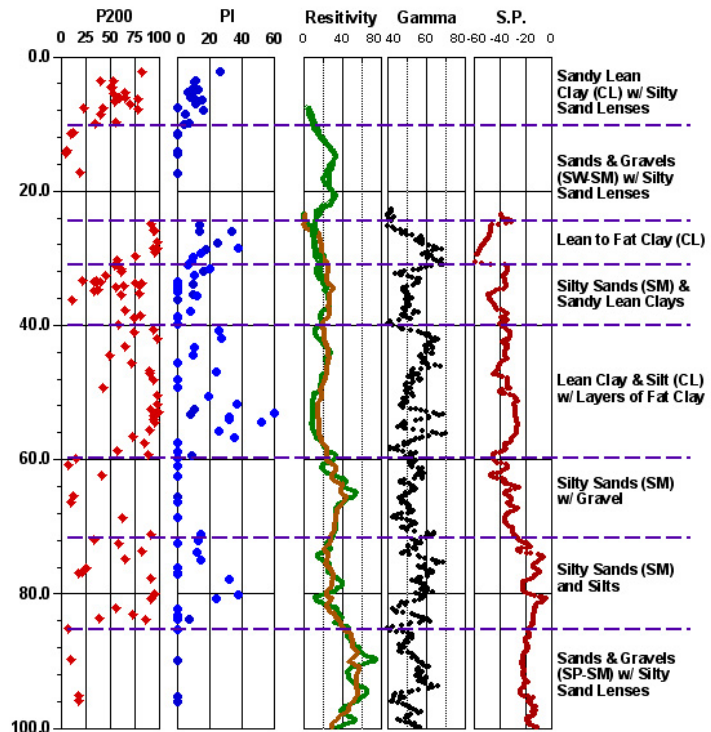
Figure 1. **Subsurface measurements for the I-10 La Cienega, CA geotechnical array site illustrating typical soil profile variability.**

The remainder of this paper describes the three GeoIndex soil groups, the data sets used for development of the GeoIndex model, the equation forms used to parameterize modulus reduction and damping curves, considerations in the development of the GeoIndex model, and a comparison of prediction error for alternative design models.

2. GEOINDEX SOIL CLASSES

The use of three broad classes of soils is central to the GeoIndex model formulation, and viewed as an appropriate balance between the competing needs for model simplicity and that of capturing significant differences between soils. Similar to the default model in SHAKE91 [5], the distinct behavior of "sand" and "clay" are recognized. However, the GeoIndex model also recognizes clear trends in dynamic properties with plasticity described by Vucetic and Dobry [4]. Table 2 defines the three GeoIndex soil classes. Class "1-PCA" is defined as primarily coarse-grained soils having 30% fines content or less and any amount of plasticity. Soils with more than 30% fines are considered to have a fine-grained matrix that governs behavior. These are separated into two groups, "2-FML" and 3-FMH", on the basis of low (<=15%) and high (>15%) plasticity index, respectively. The GeoIndex model is intended for use with

relatively common soils such as sands, silts, and clays of low to moderate plasticity that were sampled within the testing program described in section 3. The GeoIndex model should not be used for application to rock, or thick deposits of gravel, very high plasticity soils (PI>50), highly overconsolidated soils (OCR>4), or highly organic soils and peat. For these special cases, the literature should be consulted.

Table 2 – Definition of Three GeoIndex Soil Classes

GeoIndex Abbreviation	GeoIndex Soil Description	Passing #200	Plasticity Index
1 - PCA	Primarily Coarse – All Plasticity Values	<=30%	All
2 - FML	Fine-Grained Matrix– Lower Plasticity	>30%	<=15%
3 - FMH	Fine-Grained Matrix– Higher Plasticity	>30%	>15%

Note: **The GeoIndex model is *not* intended for application to rock, or thick deposits of gravel, very high plasticity soils (PI>50), highly overconsolidated soil (OCR>4), or highly organic soils and peat.**

3. LABORATORY TEST DATA SETS

The laboratory test data set used in the development of the GeoIndex model is summarized in Table 3 and includes testing of 154 natural soil specimens obtained from 28 sites and tested at two independent university laboratories using two different types of testing apparatus. Testing of these specimens was performed under the sponsorship of 4 related programs:

1) The Electric Power Research Institute (EPRI) initiated a program of applied geotechnical research after the 1989 Loma Prieta earthquake that included in-depth geotechnical investigations at three strong-motion recording sites. This research included laboratory testing of dynamic properties on 28 natural specimens by UT, and these data are summarized in an extensive report published in 1993 [9]. The EPRI program established an important precedent for subsequent investigations.

2) The 1994 Northridge earthquake provided the impetus for the initial phase of the ROSRINE project [11,12] under the sponsorship of Caltrans, NSF, and EPRI that in turn spawned a series of subsequent phases with additional partners and sponsors (see http://geoinfo.usc.edu/rosrine/). For dynamic properties characterization, the ROSRINE program adopted a strategy to use the unique and complementary capabilities of two testing labs, UT and UCLA, to extend the range of data. The RCTS equipment at UT could apply very high pressures, thus allowing testing of samples acquired at large depths to provide constraints for development of depth-dependent models. The DSDSS device [12] at UCLA offered new capabilities to significantly extend the range of testing strain over that attainable with RCTS equipment, thus providing means to constrain near-surface models for a full range of design applications. By 1998, the first two phases of ROSRINE produced laboratory data for 67 natural soil specimens obtained from 12 sites including an extensive program of testing at the La Cienega deep vertical array site. The UCLA and UT findings are reported by Tabata and Vucetic [13] and Darendeli and Stokoe [14], respectively.

3) The PEER-Lifelines (PEER-LL) partnership, sponsored by Caltrans, the California Energy Commission (CEC), and the Pacific Gas and Electric Company (PG&E), got underway in 1999 to pursue common-interest applied ground-motion research. One element of PEER-LL was to extend the site characterization efforts at strong motion recording sites initiated under ROSRINE including additional laboratory testing for dynamic properties by both UT and UCLA. These tests were largely linked with Phase 5b of ROSRINE field investigations, but were performed separately under projects 2B01/02 of PEER-LL. One objective of these investigations was to

Table 3 – Natural Soil Specimens Tested at UT and UCLA Used in Development of GeoIndex Model

Testing Program	Site	UT RCTS Tests		UCLA DSDSS Tests	
		Samples Tested	Sample Depths [m]	Samples Tested	Sample Depths [m]
EPRI '93	Gilroy #2	12	3, 6 (2), 15, 26 (2), 37, 37, 52, 64, 106, 128	0	na
	Lotung SMART-1 SMR Array	8	6, 11, 18, 25, 29, 35, 41, 45	0	na
	Treasure Island SMR Array	8	5, 9, 18, 27, 34, 40, 52, 71	0	na
ROSRINE Phases 1&2	Arleta	2	15, 31	1	7
	Dayton	0	na	3	4, 8, 16
	E. Sylmar Conv.	0	na	2	7, 16
	Kagel	4	9, 31, 65, 92	0	na
	La Cienega SMR Array	16	3, 5, 6 (2), 8, 28, 34, 36, 52, 95, 107, 125, 150, 186, 218, 241	7	5 (2), 6, 7, 8 (2), 34
	Newhall	2	21, 62	1	17
	Potrero-1	4	2, 9, 16, 31	0	na
	Rinaldi	5	2, 8, 11, 15, 21	2	2, 5
	Saturn (part 1)	0	na	2	4, 16
	Sepulveda VA	8	2, 3 (2), 14, 17, 37, 59, 86	0	na
	Obregon (part 1)	0	na	3	6, 15, 16
	Tarzana (part 1)	0	na	5	4, 7, 10, 13, 16
PEER-LL 2B01/02 ROSRINE Phase 5b	Gilroy #3	2	56, 109	1	5
	Halls Valley	2	2, 16	3	2, 5, 15
	Joshua Tree	2	72, 100	1	13
	LA Bulk Mail	5	5, 15, 51, 63, 81	2	5, 16
	Lake Hughes	1	2	0	na
	Meloland OC SMR Array	7	6, 9, 37, 61, 79, 115, 134	4	6, 9, 18, 29
	Obregon (part 2)	1	31	3	16, 21, 27
	Saturn (part 2)	1	31	0	na
	Tarzana (part 2)	2	9, 13	0	na
	Yermo	2	61, 81	1	25
NUPEC Kajima NFE Project ROSRINE Phase 5a	Corralitos	3	3, 10, 46	1	58
	Desert Hot Spr.	0	na	2	14, 26
	Devers	1	26	0	na
	El Centro #7	2	16, 101	4	16, 31, 52, 69
	Gilroy #6	2	3, 16	0	na
	N. Palm Springs	3	17, 46, 72	1	29
Summary	28 Sites	105 RCTS Tests	RCTS Depth Range: 2-241 m	49 DSDSS Tests	DSDSS Depth Range: 2-69 m

available from previous phases. Under PEER-LL 2B01/02, dynamic properties were measured on an additional 40 natural field samples obtained from 10 sites. 36 of the samples came from seven sites drilled under ROSRINE-5b, including an extensive investigation of the Meloland deep array site in the Imperial Valley. The remaining 4 samples were plastic soils obtained from three sites drilled under ROSRINE-1&2. The PEER-LL 2B01/02 project is summarized by Anderson [15] with UCLA and UT data presented in attachments prepared by Tabata and Vucetic [16] and by Stokoe et.al. [17], respectively.

4) The Kajima Corporation of Japan pursued advanced site investigation work through its Near-Field Earthquake (NFE) project, including studies of US SMR sites by the same team of field and laboratory investigators involved in the ROSRINE program. Recognizing common interests and the benefits of collaboration, a data-sharing partnership was established that is also referred to as ROSRINE-Phase 5a. The NFE investigations have yielded dynamic properties measurements on 19 samples taken from six sites. The Kajima data are summarized in a report to NUPEC of Japan [18].

Overall, the data set considered in the development of the GeoIndex model includes 154 natural soil samples obtained at 28 sites at depths ranging from 2-241 meters. Of these, 105 and 49 samples were tested in RCTS and DSDSS equipment, respectively.

Distributions of the two index properties used in the GeoIndex classification scheme are presented in Fig. 2. These data show broad ranges of both fines content and plasticity. A significant number of the samples are non-plastic, and the remaining samples have a varied plasticity that rarely exceeds 45%.
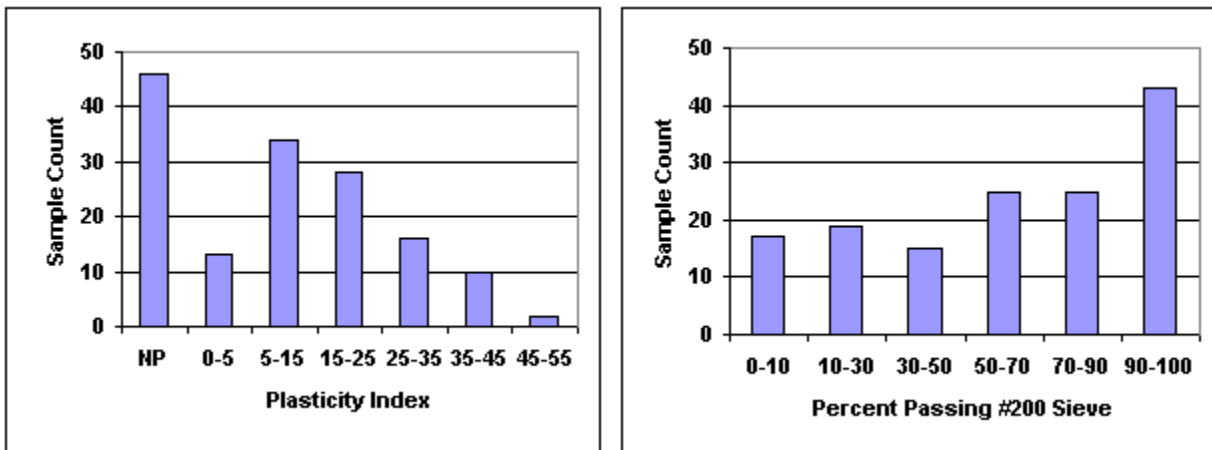
Figure 2. Distribution of index properties for samples used in development of GeoIndex model.

The GeoIndex scheme for classification of soils outlined in Table 2 is designed to capture from a limited data set the significant differences in soil types as related to dynamic properties behavior, and yet to maintain a clear and simple scheme that can be readily applied in practice. The distribution of tested samples by depth and GeoIndex soil class is presented in Table 4. Overall, the testing programs have provided a reasonably balanced set of data among the three classes, though the data clearly becomes increasingly sparse with depth due to drilling cost.

Table 5 provides summary statistics on the index properties used as classification criteria, and illustrates that the three GeoIndex groups are distinct. Soils classified as '1-PCA' tend to have both low fines content and plasticity, and are typified by soils that would classify as SW, SP, SM, and SC according to the Unified Soil Classification (USC) system [ASTM D-2487]. At the other extreme, soils classified as '3-FMH' generally have very high fines content, higher plasticity, and are comprised largely of soils that would classify by USC as CH, CL, MH, and some SC's having fines contents approaching 50%. Soils classified as '2-FML' are soils that have a large proportion of non-plastic to low-plasticity fines, and tend to classify by USC as CL, ML, and SM. The fines content for this group varies most widely as reflected in the large standard deviation. Although any simplified scheme is invariably somewhat crude,

the proposed GeoIndex scheme is clearly defined and appears to yield distinctly different soil types. Perhaps the most difficult criteria to define involved cases where plastic fines in the range of 15%-50% were encountered. The selection of P200 as the primary classification criteria over PI, and the value of P200=30% as a boundary are largely based on judgment. Future investigations should examine whether these criteria could be optimized.

Table 4 – Distribution of Samples by Depth and GeoIndex Soil Class

Depth Range [m]	GeoIndex Class		
	1-PCA	2-FML	3-FMH
0-10	10	23	18
10-20	7	8	16
20-40	10	12	9
40-80	7	10	6
80-160	7	4	4
> 160	0	2	1
Total Samples in Class:	41	59	54

Table 5 – Summary Statistics on Index Properties for Each GeoIndex Soil Class

GeoIndex Class	Passing #200			Plasticity Index		
	Median	Mean	Sigma	Median	Mean	Sigma
1-PCA	11	14	10	0	2	7
2-FML	64	66	20	8	7	5
3-FMH	95	89	15	26	28	10

Laboratory test results for each of the 154 tests were compiled into a database and used for the analyses herein. All data for 126 of the samples tested under sponsorship of ROSRINE, PEER-LL, and Kajima are publicly available for download in electronic tabular form on the ROSRINE web site (http://geoinfo.usc.edu/rosrine/).   Test results for the 28 samples from the EPRI-'93 work were not available in either electronic or tabular form [19], so test results for each of these samples were digitized from report graphs. These data, and the derived curve-fit parameters, undoubtedly will be somewhat less precise, though are considered fully acceptable in defining essential features of the test results used in subsequent analyses.

4. CURVE FIT PARAMETERS FOR INDIVIDUAL TEST RESULTS

Each test result consists of laboratory-measured values of modulus, normalized modulus, and damping ratio as a function of strain. Curves fits have been established for each set of normalized modulus and damping ratio curves using equations outlined by Darendelli et.al. [1, 2]. Each normalized modulus (G/G_m) versus shear strain (γ) curve has been fit with a 2-parameter model as follows:

$$\frac{G(\gamma)}{G_m} = \frac{1}{1+\left(\dfrac{\gamma}{\gamma_{ref}}\right)^{\alpha}}$$
(Equation 1)

The two normalized-modulus curve-fit parameters are:

γ_{ref} = reference strain that defines the location of the hyperbolic curve on the strain axis

α = shape parameter that modifies the curvature of the hyperbolic curve

Each damping ratio (D) versus shear strain (γ) curve is also fit with a 2-parameter model as follows:

$$D(\gamma) = D_{min} + \beta * D_{Masing}(\gamma) * \left(\frac{G(\gamma)}{G_m}\right)^{0.1}$$

(Equation 2)

Where

D_{Masing} = damping ratio calculated using Masing assumptions

The two damping ratio curve-fit parameters are:

D_{min} = minimum damping ratio at low strain

β = adjustment constant to scale Masing damping (D_{Masing}) to experimental data.

D_{Masing} is the ratio of dissipated energy to stored strain energy of a hysteresis loop that is a function of the G/G_m backbone curve and its shape parameter (α). Following Darendelli, D_{Masing} can be calculated in closed form solution for α=1, then approximated for other values of α using a polynomial expression as follows:

$$D_{Masing,\ \alpha=1.0}(\gamma)[\%] = \frac{100}{\pi}\left[4\frac{\gamma - \gamma_r \ln\left(\frac{\gamma + \gamma_r}{\gamma_r}\right)}{\dfrac{\gamma^2}{\gamma + \gamma_r}} - 2\right]$$

(Equation 3)

and the polynomial approximation for other values of α is:

$$D_{Masing} = c_1 D_{Masing,\ \alpha=1.0} + c_2 D_{Masing,\ \alpha=1.0}^2 + c_3 D_{Masing,\ \alpha=1.0}^3$$

(Equation 4)

Where
$c_1 = 0.2523 + 1.8618a - 1.1143a^2$

$c_2 = -0.0095 - 0.0710a + 0.0805a^2$

$c_3 = 0.0003 + 0.0002a - 0.0005a^2$

These curve-fit models for normalized modulus and damping as a function of strain are first used to explore trends in the individual test results and to establish the presence of depth and soil-type dependence in the data. Then, these same forms are used in regressions of all data within a specified depth and soil-type bin to establish target values of GeoIndex model coefficients.

5. OBSERVED TRENDS BETWEEN DIFFERENT MEASUREMENT TECHNIQIUES

An important consideration in the use of this data set is to recognize any systematic differences in results between different testing techniques. One RCTS test typically yields 3 sets of 'test results' or 3 sets of laboratory-measured modulus reduction and damping curves. One test result is reported from operation of the RCTS device in resonant column mode, and two sets are reported from operation in torsional shear mode, one each from the first and tenth loading cycle. The resonant column mode operates at frequencies typically in the 30 – 100 Hz range, while torsional shear testing is performed in

the 0.5 – 2 Hz range. All RCTS tests are performed on tall cylindrical samples confined isotropically and loaded rotationally. In contrast, the DSDSS test is performed on cylindrical disc samples confined under K_o conditions and loaded in translation at frequencies in the 0.1 – 1 Hz range. These differences in confinement, geometry, load path, and testing frequency could be expected to lead to systematic differences in laboratory-measured properties that are briefly explored here.

The strain level achieved by the different test equipment and testing modes is notable and has impact on how the data are used to define the non-linear curves. Table 6 summarizes the number of tests available for analysis at different levels of soil non-linearity as measured by normalized modulus. It is readily apparent that the DSDSS test provides definition of the curve over a more complete range of strain. The DSDSS tests routinely define the modulus reduction curve beyond several percent strain. In contrast, roughly half of the RC tests achieve a modulus reduction value of 50%, and TS tests rarely achieve that level. For purposes of examining trends in the data, a screening threshold value for minimum measured normalized modulus of 0.75 has been set for consideration of curve-fit parameters that require definition of curve shape (i.e. γ_{ref}, α, β). However, all data are used to examine trends in low strain laboratory measurements (i.e. D_{min}, G_{max}).

Table 6 – Distribution of Test Results by Test Type and Strain Level Achieved

Minimum Measured G/Gm	Number of Test Results Available (PEER-LL, ROS, & Kajima Sets only)				
	Total	DSDSS	RC*	TS1*	TS10*
<1.0	364	49	112	102	101
<0.9	316	49	112	76	79
<0.8	260	49	110	49	52
<0.7	218	49	106	30	33
<0.6	177	49	94	17	17
<0.5	137	49	67	9	12
<0.4	97	48	40	4	5
<0.3	58	45	13	0	0
<0.2	45	44	1	0	0

* Includes tests of same specimen at multiple confining pressures

Table 7 summarizes findings regarding systematic differences between RC and TS test results on the same soil specimens. These findings are based on a subset of 28 RCTS tests on 24 samples where results for all three modes, RC, TS1, and TS10, were reported and for which strain levels achieved the screening threshold of G/Gm=0.75. The statistics in Table 7 are reported as ratios of model parameters to eliminate the effect of differences between soil samples and focus on systematic trends between results of different testing modes. These data show that TS10 and TS1 results are virtually identical with the possible exception of a slight decrease in high-strain damping, as reflected in beta, of TS10 results relative to TS1 results. However, significant differences are shown to exist between RC and TS results. As previously discussed, the RC testing mode is capable of achieving higher levels of strain than the TS testing mode, thus providing a lower value of minimum measured modulus ratio. Other distinct trends include that the RC test yields a slightly higher (+13%) value of Gmax, a much higher value of low-strain damping (+200%), and a slightly flatter shape in the G/Gm curve as reflected by a slightly lower value for alpha (-10%) relative to TS results. The large difference in low-strain damping is often attributed to frequency effects, although it is also possible that there are unaccounted energy losses in the equipment when operating at resonance. Less clear trends in Table 7 include possible small increases in both reference strain and beta, though these changes are clearly within the range of scatter, and may be related to the shape changes.

Table 7 – Comparison of RC, TS1, and TS10 Results from Identical Samples in the RCTS Device

Model Parameter	Ratio of TS10/TS1 (28 Tests, 24 Samples)			Ratio of RC/TS1 (28 Tests, 24 Samples)		
	Median	Mean	Sigma	Median	Mean	Sigma
Minimum Measured G/Gm	0.99	0.98	0.03	0.65	0.64	0.18
Gmax	1.00	1.00	0.00	1.13	1.17	0.13
Ref Strain	0.98	0.98	0.05	1.09	1.18	0.35
Alpha	0.98	0.98	0.05	0.88	0.91	0.11
Dmin	0.97	0.96	0.09	2.12	2.25	1.09
Beta	0.91	0.90	0.09	1.17	1.22	0.44

Table 8 extends this comparison of test methods to include DSDSS results for a unique subset of the overall data set where 'companion' samples were tested in both DSDSS and RCTS equipment. Within the overall testing program, 14 companion samples were tested in both devices, however, only 9 of the specimens passed screening criteria where all tests achieved a minimum G/Gm ratio of 0.75 or less. Ratios for RC-to-TS1 testing mode results are included in Table 8 to illustrate that results very comparable to those presented in Table 7 are achieved for the smaller data set. Ratios for TS10-to-TS1 are not repeated since these test results were nearly identical as shown in Table 7.

Table 8 – Comparison of DSDSS and RCTS Results for Companion Samples

Model Parameter	Ratio of RC/TS1 (9 Tests, 9 Samples)			Ratio of DSDSS/TS1 (9 Tests, 9 Samples)			Ratio of DSDSS/RC (9 Tests, 9 Samples)		
	Median	Mean	Sigma	Median	Mean	Sigma	Median	Mean	Sigma
Gmax	1.16	1.16	0.07	0.65	0.62	0.19	0.54	0.54	0.17
Ref Strain	1.05	1.03	0.17	1.26	1.25	0.30	1.24	1.22	0.26
Alpha	0.93	0.94	0.07	0.77	0.84	0.14	0.89	0.89	0.11
Dmin	2.80	2.52	0.73	1.89	1.90	1.17	0.78	0.81	0.39
Beta	1.24	1.28	0.59	1.19	1.17	0.23	0.97	1.01	0.29

The ratios in Table 8 reveal important differences between results of the DSDSS and the RCTS tests that are further illuminated in the paper by Anderson in this proceeding. First, the laboratory-measured Gmax value from the DSDSS is roughly half that of the RCTS tests. Nearly all Gmax values measured from laboratory testing is below field geophysical measurements of Gmax. Smaller ratios between laboratory to field modulus is often interpreted as a sign of increasing soil disturbance. It is possible that the process used in the DSDSS sample preparation that requires lateral displacement to fully seat the sample against the wire-wound confining membrane leads to a large strain cycle prior to testing. Other significant trends in Table 8 include that the DSDSS device yields higher values (+25%) of reference strain and somewhat lower values of alpha (–10% to –20%) relative to the RCTS device. Low-strain damping values measured by the DSDSS are between those measured by RC and TS, with DSDSS values closer to those produced by RC even though the operational frequencies differ greatly. Each of these differences could be associated with either sample disturbance or differences in stress path, confinement, and sample geometry.

Figure 3 illustrates systematic differences in test results stemming from the various testing devices and testing modes using the ratios presented in Tables 7 and 8. Large differences are apparent in both strain range and absolute modulus. However, the normalized modulus plots are very consistent, and in practice, differences are within the typical range of data scatter. The damping curve shows generally similar trends with somewhat lower Dmin values for TS than the other two tests. The damping

curve for DSDSS results is presented as two distinct symbols since damping values are commonly reported to only 0.1% strain, but are technically measurable with the DSDSS and occasionally reported to much higher strain values.

6. EFFECTS OF INCREASED CONFINEMENT ON MODEL PARAMETERS

Another unique subset of the UT test results are samples where dynamic properties were measured at multiple confining pressures. While only test results for confinement equal to estimated in-situ stress are used for regression of the GeoIndex model, the results for multiple confining stresses are used here to examine the relationship between confinement and dynamic properties. Within the available digital UT data (ROSRINE, PEER-LL, and Kajima), 71 sets of results were generated at a pair of confining pressures corresponding to one and four times estimated in situ stress. Of those, only 34 pairs met screening criteria of achieving a minimum G/Gm=0.75 or less with the all but 8 of those being RC tests on specimens obtained from relatively shallow depths. To eliminate effects of mixing test types, the statistics presented in Table 9 were developed from only from the 26 RC tests performed on unique samples.

Table 9 presents ratios of measured test and curve-fit parameters from tests performed at four times estimated in situ confining pressure to

Figure 3. Systematic differences in test results from RC, TS, and DSDSS tests.

that measured at estimated in situ stress for each of the three GeoIndex soil classes. These results illustrate several important trends. First, a factor of four change in confining pressure results in approximately a 100% increase in low-strain modulus for both 1-PCA and 2-FML soil types as would be expected from theory, but leads to only a 40% increase for 3-FMH. The smaller change for 3-FMH soils may be an artifact related to the set of soils tested consisting primarily of near-surface clays that may be
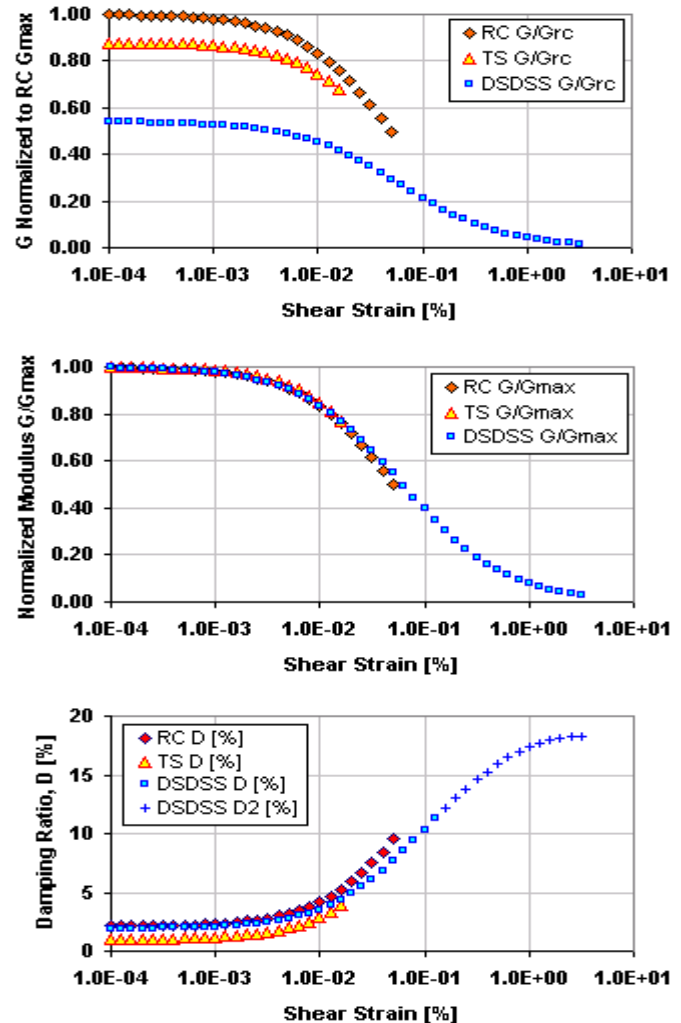
Table 9 – Effect of Increased Confining Stress on RC Results

Model Parameter	Ratio of Model Parameter Values Measured at 4* In Situ Stress / 1* In Situ Stress								
	1-PCA (6 Tests, 6 Samples)			2-FML (9 Tests, 9 Samples)			3-FMH (11 Tests, 11 Samples)		
	Median	Mean	Sigma	Median	Mean	Sigma	Median	Mean	Sigma
Gmax	2.12	2.07	0.41	2.01	2.08	0.26	1.37	1.40	0.24
Ref Strain	1.29	1.34	0.23	1.53	1.49	0.24	1.14	1.13	0.28
Alpha	1.10	1.09	0.05	1.11	1.08	0.10	1.07	1.19	0.24
Dmin	0.82	0.84	0.09	0.79	0.88	0.20	0.88	0.92	0.22
Beta	1.11	1.12	0.12	0.94	1.07	0.44	0.97	0.98	0.15

overconsolidated. Other significant trends in Table 9 include that increasing pressure leads to a small increase in the shape parameter (alpha) and a small decrease in low-strain damping (Dmin). Typical impacts of increased confining pressure are illustrated in Fig. 4.

The results in Table 9 suggest a possible relationship between changes in low-strain modulus and reference strain similar to one suggested by Pyke [1998]. These data suggest that the ratio of reference strain appear to be approximately proportional to either the square root of the ratio in modulus, or the velocity ratio as:

$$\frac{\gamma_{r,2}}{\gamma_{r,1}} \propto \sqrt{\frac{G_{m,2}}{G_{m,1}}} \propto \frac{v_{s,2}}{v_{s,1}} \qquad \text{(Equation 5)}$$

This correlation is examined further in Table 10 that presents statistics on the velocity ratio and "normalized reference strain ratio (NRSR)" calculated for each of the pressure-pair samples considered in Table 9. The NRSR value is calculated as the reference strain ratio divided by the velocity ratio on an individual sample basis. The mean and median statistics in Table 10 suggest that NRSR is near unity for all soil types in the data set. This suggests that pressure-induced changes in reference strain could be directly proportional to pressure-induced changes in shear-wave velocity. This concept needs to be further evaluated for larger data sets and using a wider range of confining pressure ratios. This concept might also be considered as a means to compensate for possible disturbance-related differences in low-strain modulus measured in the laboratory and in the field.
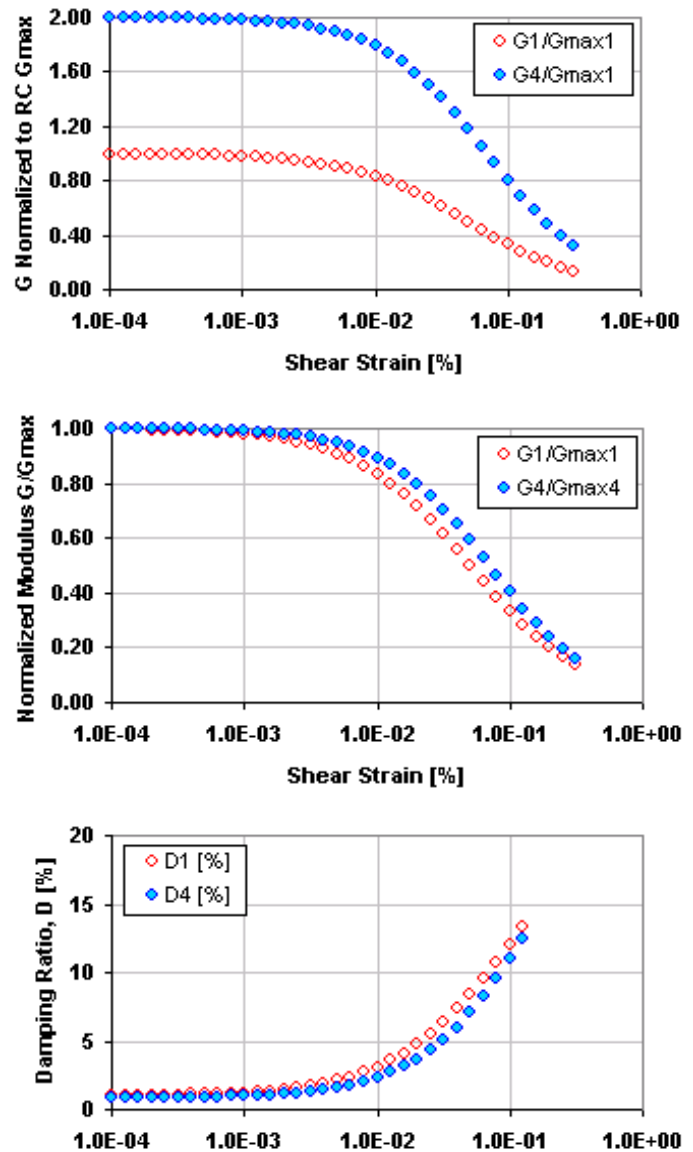

Figure 4. Typical effect of increasing confinement by a factor of 4 (1-PCA and 2-FML soils)

Table 10 – Correspondence Between Velocity Ratio and Reference Strain Ratio

Model Parameter	Ratio of Velocity and Normalized Reference Strain Values Measured at 4* In Situ Stress / 1* In Situ Stress								
	1-PCA (6 Tests, 6 Samples)			2-FML (9 Tests, 9 Samples)			3-FMH (11 Tests, 11 Samples)		
	Median	Mean	Sigma	Median	Mean	Sigma	Median	Mean	Sigma
Velocity Ratio	1.45	1.43	0.15	1.42	1.44	0.09	1.17	1.18	0.10
Normalized Reference Strain Ratio	0.95	0.93	0.10	0.99	1.04	0.17	1.00	0.96	0.22

7. DEVELOPMENT OF THE GEOINDEX MODEL, v1

The most important outcome of these analyses of laboratory data is the development of a practical model for specification of dynamic properties for engineering practice. This section describes the development of a depth-dependent model for the curve-fit parameters described in Section 4, using the subset of test results described in Section 3 for confinement at estimated in situ stress, and the GeoIndex soil classification scheme described in Section 2. Model development has been an iterative process involving both statistical analyses and reasoned judgments. The process used to develop and smooth the GeoIndex model is outlined below, followed by presentation and discussion of the fit of the data by model predictions.

Model development started with statistical regression of curve-fit coefficients for the normalized modulus data for each of three GeoIndex soil groups and six depth bins. Initial analyses of average and median curve-fit parameters for each depth and soil type bin showed little dependence of the shape parameter (alpha) on depth, but a significant dependence on both testing technique and soil type. UCLA data had consistently lower alpha values relative to UT data, reinforcing the trends presented in Table 8. When considered separately, neither UCLA nor UT data showed significant depth dependence, but both showed similar trends between soil types. The lowest alpha value is associated with 1-PCA soil (relatively clean sands) and the highest with 3-FMH soil (higher PI clays). Subsequent regressions of the entire normalized-modulus data set fixed alpha to be a constant value over all depths ranges for each of the three soil types, and only reference strain was allowed to vary with depth. The final alpha values from regression of the combined data set at in situ stress are 0.85, 0.90, and 0.98 for 1-PCA, 2-FML, and 3-FMH soils, respectively.

The same regression of the combined data set at in situ stress yielded the reference strain values shown in the left-hand figure of Fig. 5. Two 'best' estimates plus confidence bounds are presented for each of the three soil types for each of 5 depth bins. Soil types were combined for the bottom depth bin due to the paucity of data. The two 'best' estimates are for all test types (dark solid symbol) and for UT data only (light solid symbol). A separate estimate is presented for the UT data to allow for consideration of trends with depth independent of test type. As previously discussed, the UCLA data yields a larger value of reference strain, and the mixture of UCLA and UT data varies with depth.
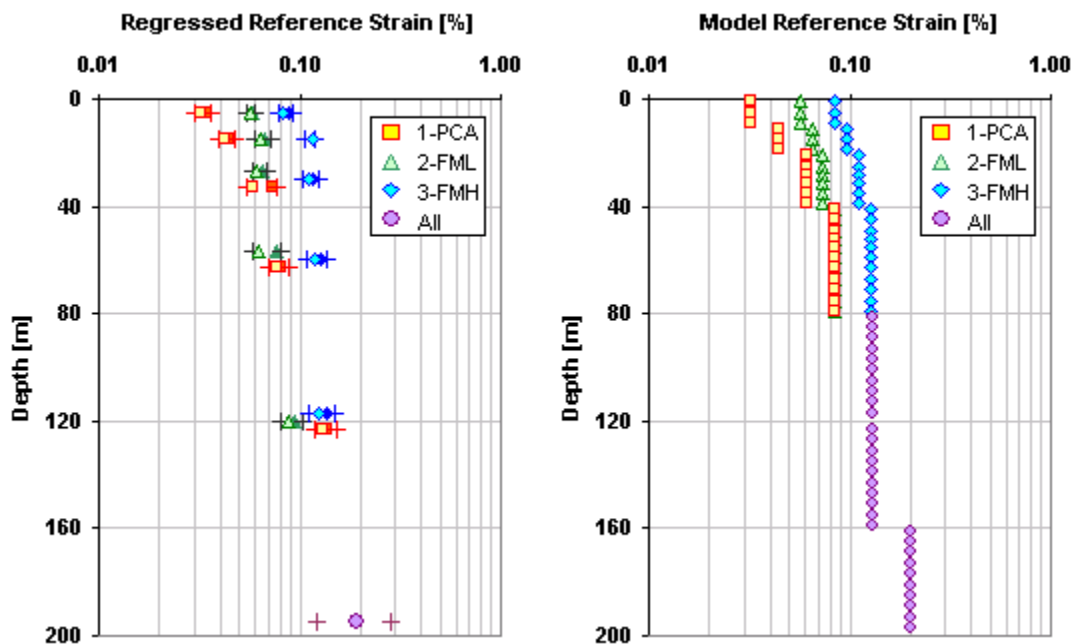

Figure 5. Development of reference strain model – regressed values (left) and final model (right).

The data in Fig. 5 clearly show that reference strain is depth dependent, and that the three soil types are distinct near the ground surface. At shallow depths, 1-PCA (sandy) soils have the lowest values of reference strain, 3-FMH (higher PI clays) the highest, and 2-FML (silts and low-PI clays) are in the middle. As depth increases, reference strain values for 1-PCA soils increase rapidly, while those for 3-FMH increase slowly until they merge in the 5th depth bin (plotted near 120 m). The depth trend for 2-FML soils is somewhat perplexing. At shallower depths, these soils are distinctly in the middle of the range for the other soil types. However, the data suggest moderately lower values of reference strain than either of the other soil types in the 4th and 5th depth bins. This behavior is counterintuitive to the authors who expected this soil to remain bracketed by the other two soils over the entire depth range. It is unclear whether this counterintuitive trend is real or indicative of testing problems, an artifact of the particular mixture of samples within this bin, soil disturbance effects, or a flaw in the GeoIndex soil groupings. Additional testing may be required to resolve this issue.

The right-hand plot in Fig. 5 presents the interpreted final values of reference strain for the GeoIndex model. The model for 1-PCA soils closely follows the regression results. The model for 3-FMH soils includes relatively minor smoothing through the 2nd and 3rd depth bins to provide a gradual increase with depth. The model for soil types 1-PCA and 3-FMH are merged for the lower two depth bins as suggested by the data. The values for 2-FML soils were also smoothed somewhat near surface. The most significant judgment incorporated into the model is that 2-FML soils are not allowed to cross below the 1-PCA line as suggested by the data. Rather, The 2-FML model is merged with the 1-PCA model at the 4th depth bin (40-80 m) and combined with all other soils at greater depths. The values shown in the right-hand plot of Fig. 5 plus the constant values for shape parameter (alpha) comprise the complete model for the normalized modulus curves. The values are tabulated at the end of the section.

Development of the damping curve model involved a similar series of steps. First, low-strain damping (Dmin) was examined independently of higher-strain data. Statistics were developed separately for each testing method since there are distinct differences as described in Section 5 and in Tables 7 and 8. The left-hand plot of Fig. 6 presents bin-specific averages for each test type. Soil type is denoted by symbol shape. TS-1 and TS-10 data are plotted as the two larger filled symbols of each shape, RC data is plotted as the smaller filled symbol, and DSDSS data are plotted as the smaller open symbol. The TS data shows a relatively smooth trend indicating depth dependence, while the RC data is systematically higher and more scattered. DSDSS data is limited to the near surface.
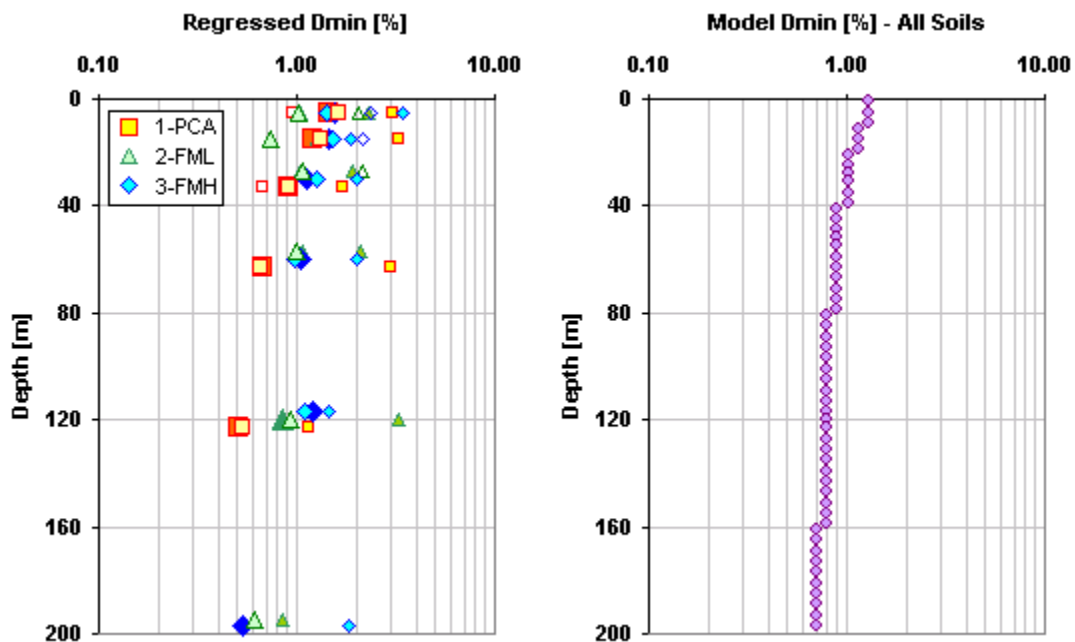

Figure 6. Development of Dmin model – regressed values (left) and final model (right).

The right-hand plot in Fig. 6 presents the final model that incorporated these data as well as several key assumptions. The model relies heavily upon TS data since that measurement is available at all depths, provides the least scatter, and is arguably a more reliable measurement than RC. Even within the TS data, it is difficult to establish unambiguous trends between soil types. A possible trend is that the 1-PCA soil moves systematically toward lower damping at depth while the other two soil groups show less depth dependence. However, this distinction between soil types is muted and certainly within the data scatter. Therefore, a decision was made to model all soils together, and incorporate a small amount of depth dependence as shown in the right-hand plot.

The final model parameter to be established is the 'beta' term in equation 2 that scales a function of Masing damping to the data. Table 11 details results of regressions for both soil type and depth, and for depth alone. Testing method was not considered. No discernable trend is apparent on the basis of soil type. When depth alone is considered for all soil types, a smooth trend appears, though no physical basis is readily apparent to explain the variation. Therefore, for simplicity, a single constant value of beta of 0.62 is assigned to all soil types and depths in the GeoIndex model. Finally, variations on the the 0.1 power on the G/Gm adjustment term in equation 2 were considered, but little benefit was derived from using a value different from that proposed by Darendelli and Stokoe.

Table 11 – Regression Results for 'Beta' Term in Damping Curve Fit Equation.

Depth Range	All Soil Types	GeoIndex Soil Type		
		1-PCA	2-FML	3-FMH
0-10	0.59	0.59	0.57	0.62
10-20	0.63	0.70	0.52	0.55
20-40	0.70	0.63	0.77	0.74
40-80	0.65	0.69	0.69	0.54
80-160	0.47	0.28	1.14	0.48
> 160	0.46	NA	0.41	0.90
All Depths	0.62			

Table 12 summarizes the final recommended coefficients for the GeoIndex model, version 1 that includes a depth and soil-type dependent reference strain, a soil-type dependent alpha, a depth dependent Dmin, and a constant value for beta. Tabulated GeoIndex model values for normalized modulus and damping as a function of strain are attached as an appendix to the back of this paper.

Table 12 – Recommended Coefficients for GeoIndex Model, Version-1

GeoIndex Model	1-PCA Soil				2-FML Soil				3-FMH Soil			
Depth [m]	Ref. Strain	Alpha	Dmin	Beta	Ref. Strain	Alpha	Dmin	Beta	Ref. Strain	Alpha	Dmin	Beta
0-10 m	0.032	0.85	1.30	0.62	0.057	0.90	1.30	0.62	0.085	0.98	1.30	0.62
10-20 m	0.044	0.85	1.15	0.62	0.065	0.90	1.15	0.62	0.097	0.98	1.15	0.62
20-40 m	0.061	0.85	1.02	0.62	0.074	0.90	1.02	0.62	0.111	0.98	1.02	0.62
40-80 m	0.085	0.85	0.90	0.62	0.085	0.90	0.90	0.62	0.126	0.98	0.90	0.62
80-160 m	0.130	0.85	0.80	0.62	0.130	0.90	0.80	0.62	0.130	0.98	0.80	0.62
>160 m	0.200	0.85	0.70	0.62	0.200	0.90	0.70	0.62	0.200	0.98	0.70	0.62

Note: The GeoIndex model is *not* intended for application to rock, or thick deposits of gravel, very high plasticity soils (PI>50), highly overconsolidated soil (OCR>4), or highly organic soils and peat.
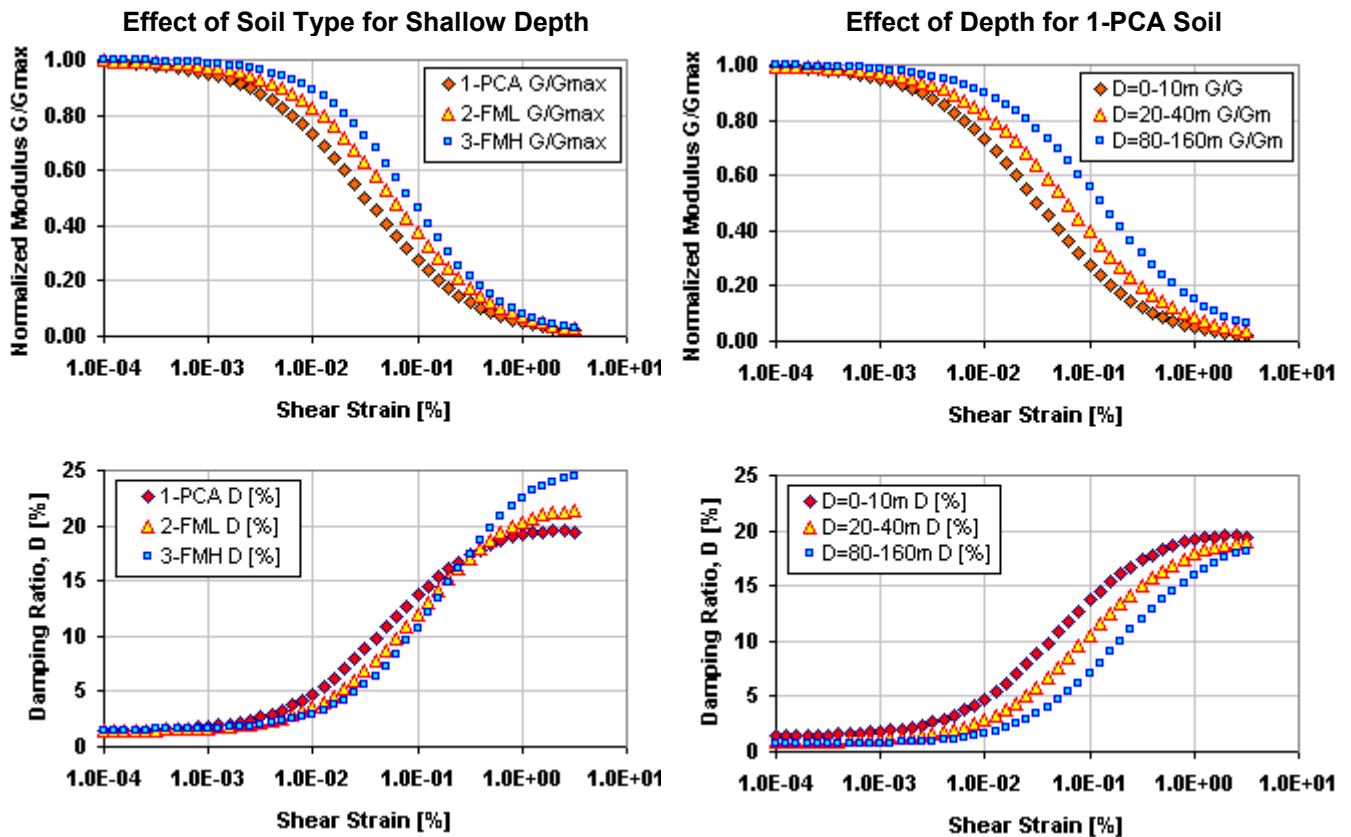
Figure 7. Illustration of GeoIndex model behavior for different soil types and depth ranges.

8. ASSESSMENT OF THE GEOINDEX MODEL, v1

Figure 7 illustrates the general behavior of the GeoIndex model. The plots on the left illustrate differences between soil types near the ground surface. The 1-PCA (sandy) curves are the most non-linear with increased linearity for 2-FML and 3-FMH soils. This trend is consistent with behavior identified by Vucetic and Dobry [4], Idriss and Sun [5], and Darendelli [1]. In addition to moving toward greater reference strain, the shapes of the normalized modulus curves vary slightly with the 3-FMH curve showing the most curvature, or most rapid rate of reduction in modulus, past the elastic threshold strain. The difference in shape is unique to this model. An interesting manifestation of the difference in curvature of the normalized modulus curves is the crossing of the damping curves at higher levels of strain. The data set for damping at this level of strain is simply too sparse to definitively support or refute the crossing, but as will be shown in subsequent plots, this trend is not unreasonable.

The plots on the right-hand side of Fig. 7 illustrate GeoIndex model behavior with depth. This figure was prepared for the 1-PCA soil which exhibits the greatest depth dependence. Only every other depth bin is plotted (bins 1, 3, and 5) for figure clarity. Here, the normalized modulus curve shape remains constant and simply shift right toward higher reference strain values with increasing depth. This trend is consistent with the EPRI model [6], the BNL model [8] and the Darendelli model [1].

The ultimate sanity check on the adequacy of a model is to compare predicted values relative to observations. Figures 8 and 9 do precisely that. Figure 8 shows all normalized modulus measurements for each of the 18 GeoIndex model bins relative to the predicted curve. From top to bottom, the plots correspond to the six GeoIndex depth bins. From left to right, the plots correspond to the three GeoIndex soil types. The overall match between prediction and data is reasonable for all bins with no obvious systematic bias. The fit for the well-populated near-surface bins is particularly satisfying, as the data appear to support the model variations in shape parameter between soil groups.
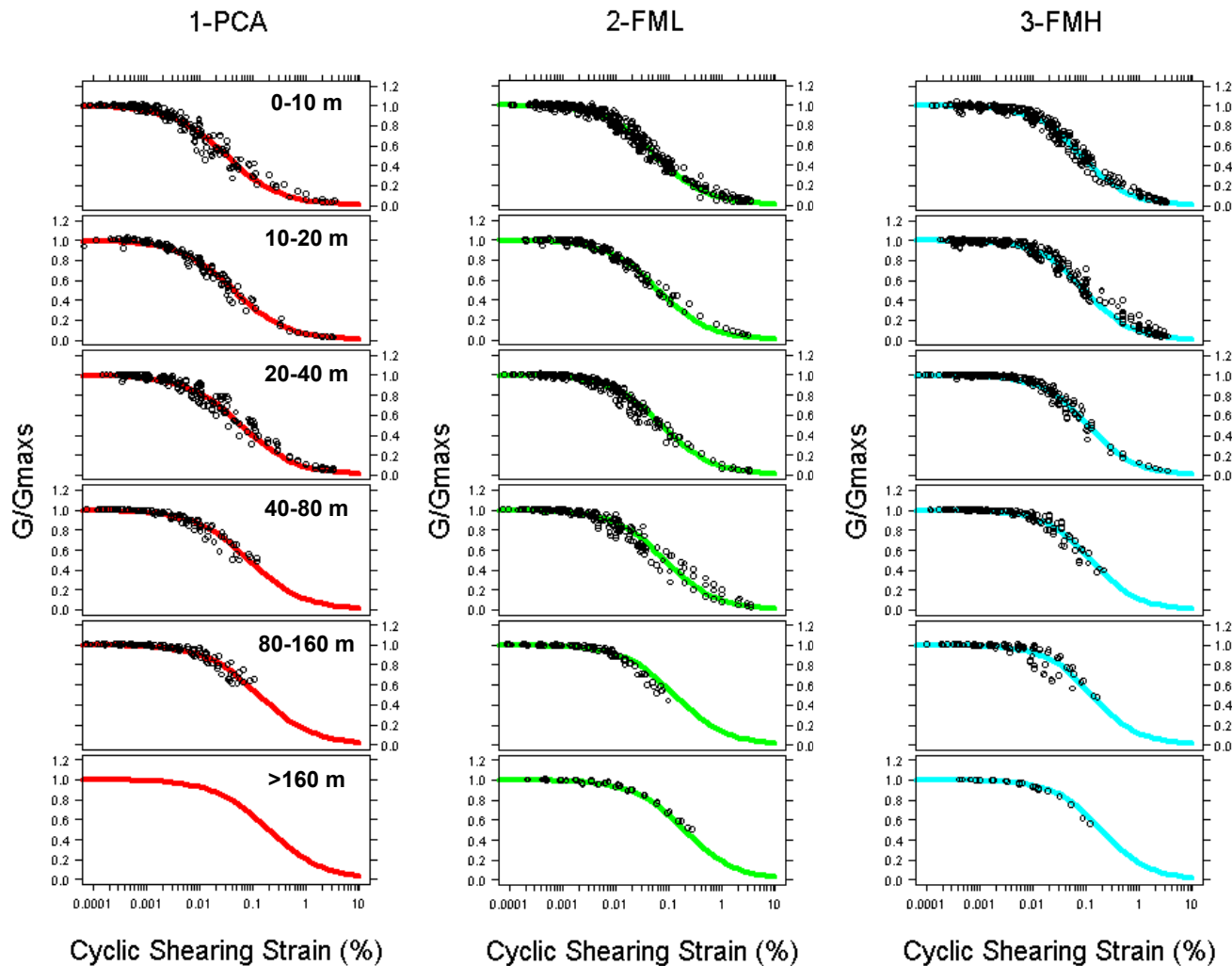
Figure 8. All laboratory-measured normalized modulus data (for confinement at estimated in situ stress) relative to GeoIndex model predictions. Top to bottom corresponds to increasing depth for the six depth bins. Left to right corresponds to 3 soil types.

Figure 9 presents the damping measurements relative to GeoIndex model predictions using the same arrangement as in Fig. 8. The plots are presented twice; the top set presents all data while the bottom set is for TS and DSDSS data only. Several trends are notable in these data. First, the model-development decision to favor the TS data is readily apparent at low strain. The bottom set of figures show a close match to the TS data, with the higher values of misfit corresponding to the DSDSS data. The top set of figures shows the RC data clearly above the model at low strain. However, the curve shape of the model captures the trend in the RC data quite reasonably. Figure 9 also highlights the paucity of data at high strain. These data also show a large degree of scatter that is insufficient to resolve clear trends between soil groups, particularly regarding whether the damping curves cross. The data also suggest that there may be a slight under-prediction of the average high-strain, though given the scatter, the model predictions are well within reason.

Figures 10 through 12 present summaries of model residuals for each GeoIndex model soil type and depth bin. Figure 10 presents residuals for normalized modulus, and Figs. 11 and 12 for damping ratio. The damping ratio data in Fig. 11 is from TS and DSDSS data at low frequencies only, while the data in Fig. 12 is from RC data at higher frequencies. The normalized modulus residuals show a slight under-prediction at high strain, primarily relative to DSDSS results since the model weighted all data types equivalently and only DSDSS data is available at high strain. The damping residuals illustrate trends already discussed that the model predicts lower values than RC measurements.
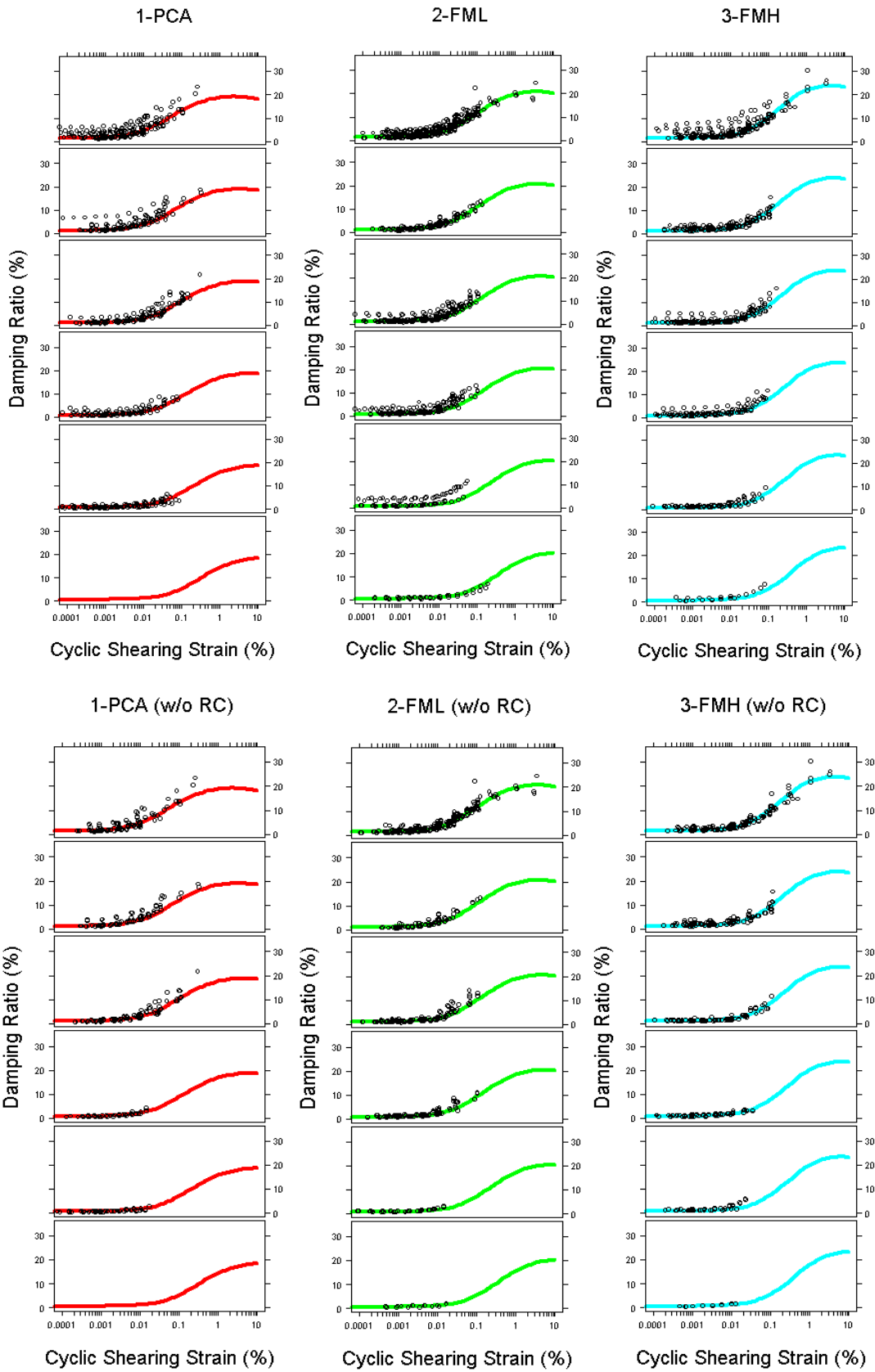
Figure 9. Laboratory-measured damping data (for confinement at estimated in situ stress) relative to GeoIndex model predictions. Top set shows data from all devices. Bottom set is for TS and DSDSS data only. Within each plot set, top to bottom corresponds to increasing depth, and left to right corresponds to 3 soil types.

9. COMPARISON OF ALTERNATE DESIGN MODELS

In this section, the data set used for development the GeoIndex model is also used to examine several alternative design models. Figures 13 through 15 present residuals for each of three models: SHAKE91 [5], Vucetic and Dobry [4] and Darendelli and Stokoe [1, 2]. For each model, each sample in the laboratory-test database was assigned dynamic properties on the basis of criteria unique to that model. Predictions were made for each sample tested at in situ confining stress, and residuals were calculated as the difference between laboratory observations and model predictions. The residuals are grouped into the six depth bins used for the GeoIndex model as a means to illuminate any bias with depth. The earlier models were developed from laboratory test results at lower confining pressures, and should not be expected to capture recently observed behavior at higher confining stresses.

To examine the SHAKE91 default model, each sample was classified as either 'sand' or 'clay' on the basis of unified soil classification criteria. Soils having up to 50% fines were classified as sands, and both silts and clays were classified as clays. The residual plots in Fig. 13 show significant bias in the normalized modulus results. Clay is strongly biased toward more linear behavior than observed for nearly all depths, and sand is somewhat too linear near surface and too non-linear at depths beyond 80 m.

To examine the Vucetic and Dobry model, each soil was classified into one of four PI groups: 0, 15, 30, or 50 based on the measured PI for each specimen. The residual plots for normalized modulus in Fig. 14a show that the PI=0 curve is somewhat biased toward too much non-linearity near surface, and strongly biased at depth. The PI=15 and PI=30 curves are fairly unbiased through 40 m, but become too non-linear at large depths. The PI=50 curves appear slightly biased toward too linear behavior.

Finally, the depth-dependent Darendelli and Stokoe model is examined. This model is formulated as a continuous function of both PI and OCR. Assignment of PI value was straightforward as this information was reported for nearly all tested specimens. However, a value for OCR was very difficult to assign where not directly reported through lab testing. Further, based on a limited number of specimens for which OCR values were reported by Stokoe et.al. [17], no consistent proxy for OCR could be identified that was not already correlated to PI (which is already a model parameter). Therefore, for this exercise, all specimens were assigned an OCR value of unity. For context, this assumption is not extreme. Of the 25 samples tested in the Stokoe et.al. study, only 5 were assigned a non-unity value. As expected, the residual plots in Fig. 15 show that the Darendelli model captures the depth dependent behavior of the laboratory test data. However, the residuals from this model are actually larger than those found using the simpler GeoIndex model for this data set. This observation is attributed to using a constant shape factor and possible added model variability associated with using PI directly as a predictor variable.

10. CONCLUSIONS

This paper synthesizes results of an extensive program of state-of-the-art laboratory testing of 154 natural soil samples obtained at 28 sites, and outlines the empirical development of a new depth and soil-type dependent GeoIndex model for practical design specification of dynamic material properties for earthquake site response analysis. Systematic differences between results of different testing equipment are identified. Laboratory RCTS results on samples tested at multiple confining pressures are used to identify a potential strategy for adjusting normalized modulus curve fit parameters to account for common discrepancies between measured field and laboratory modulus.

The GeoIndex model provides an easily implementable design tool that builds on recent concepts developed by Darendelli and Stokoe, and incorporates key features regarding both soil-type and depth dependence found in alternate earlier design models. Examination of residuals for this data set shows that the GeoIndex model achieves reasonable predictions near the surface and is unbiased with depth. Although very straightforward to apply, the prediction error for the GeoIndex model is shown to be comparable to those for the more sophisticated Darendelli model. Some earlier models still commonly used in practice show significant bias at depth toward less elastic behavior than indicated by the test data. These earlier models had been developed without the benefit of recent laboratory test results for large confining stresses, and their use should be restricted to analysis of shallow profiles.
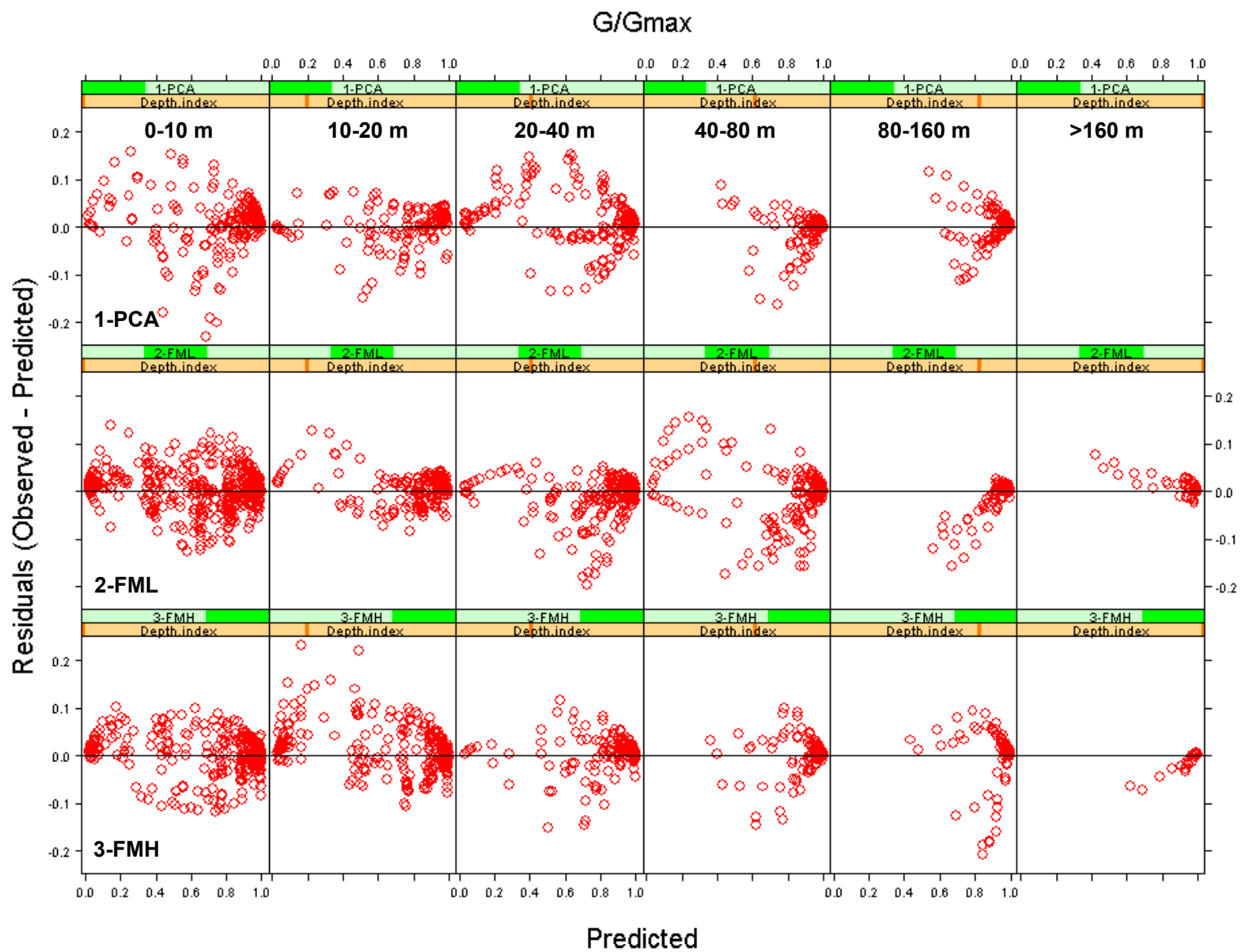
Figure 10. Residuals in normalized modulus between laboratory observations and GeoIndex model predictions.
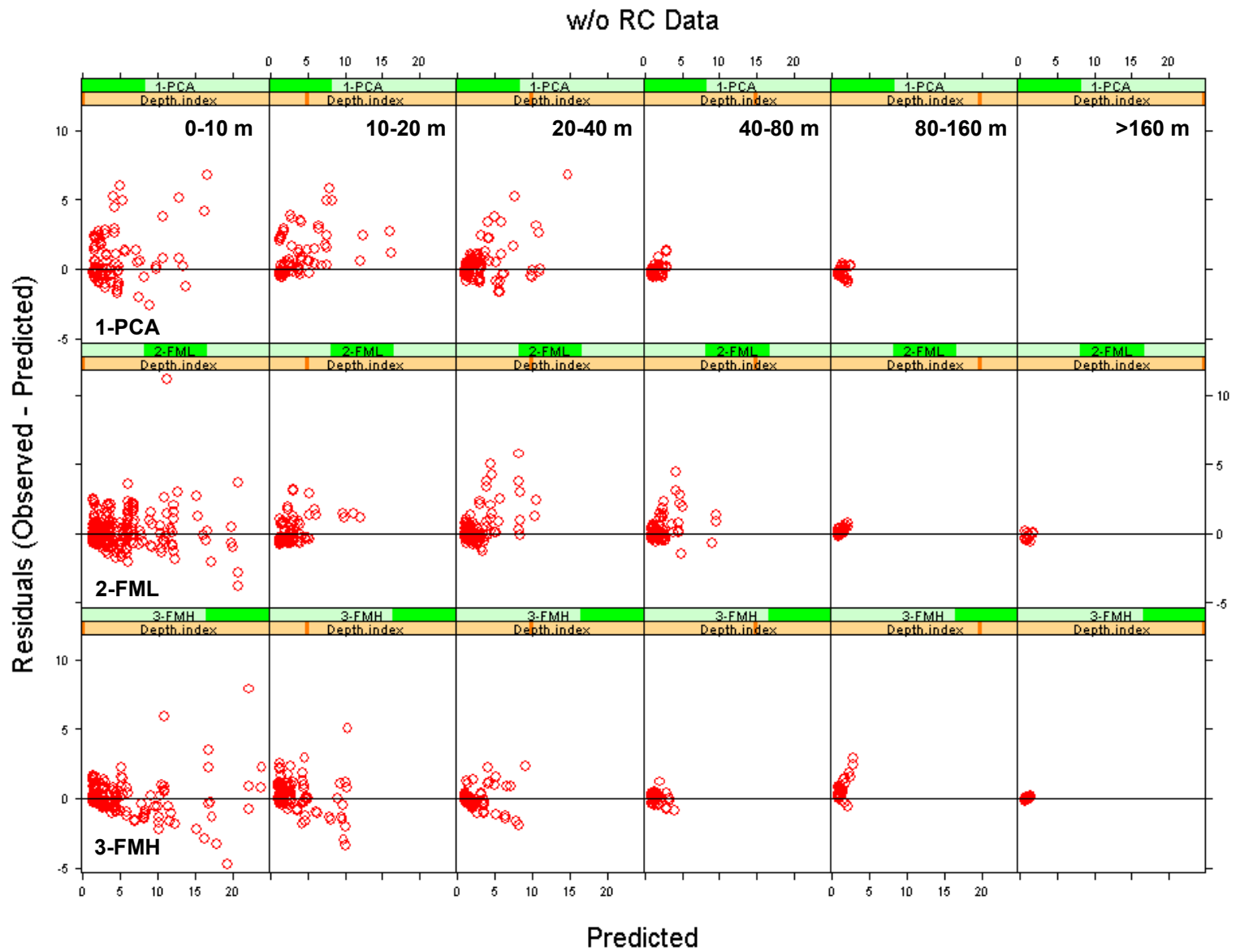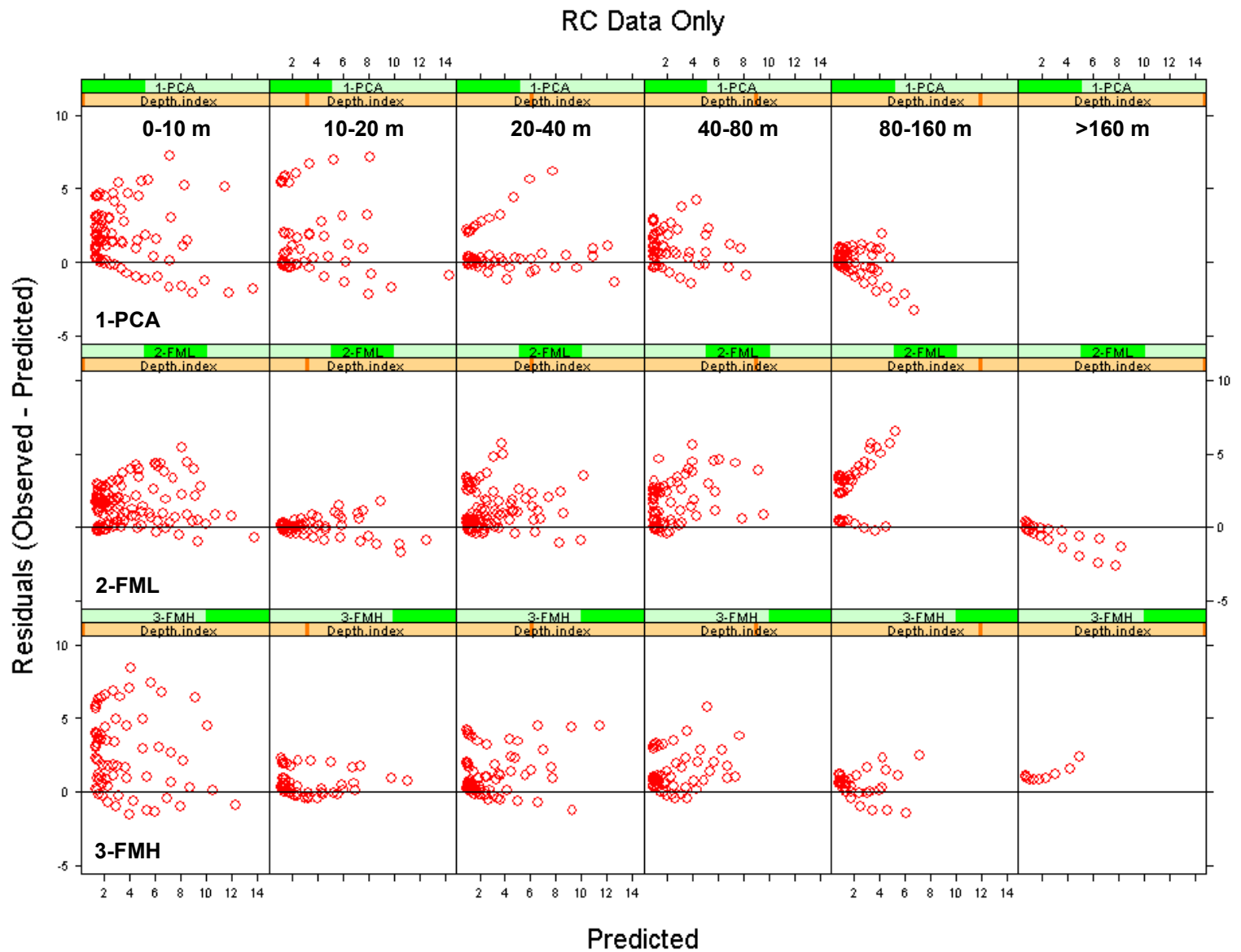
Figure 11.   Residuals in damping between TS and DSDSS laboratory observations and GeoIndex model predictions.

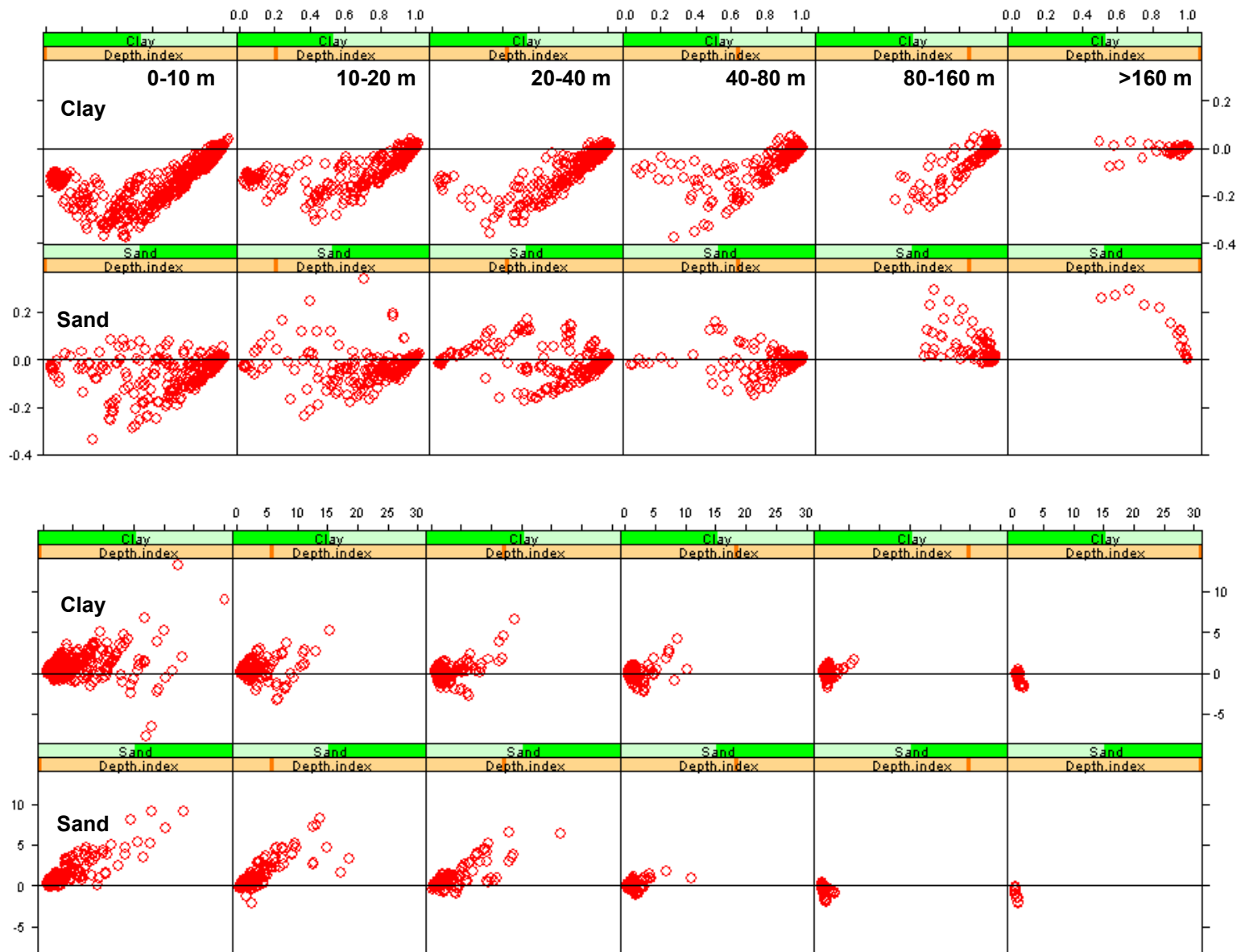**Figure 12.   Residuals in damping between RC laboratory observations and GeoIndex model predictions.**

Figure 13. Residuals in G/Gm (top) and D (bottom) laboratory observations and SHAKE91 [5] model predictions.
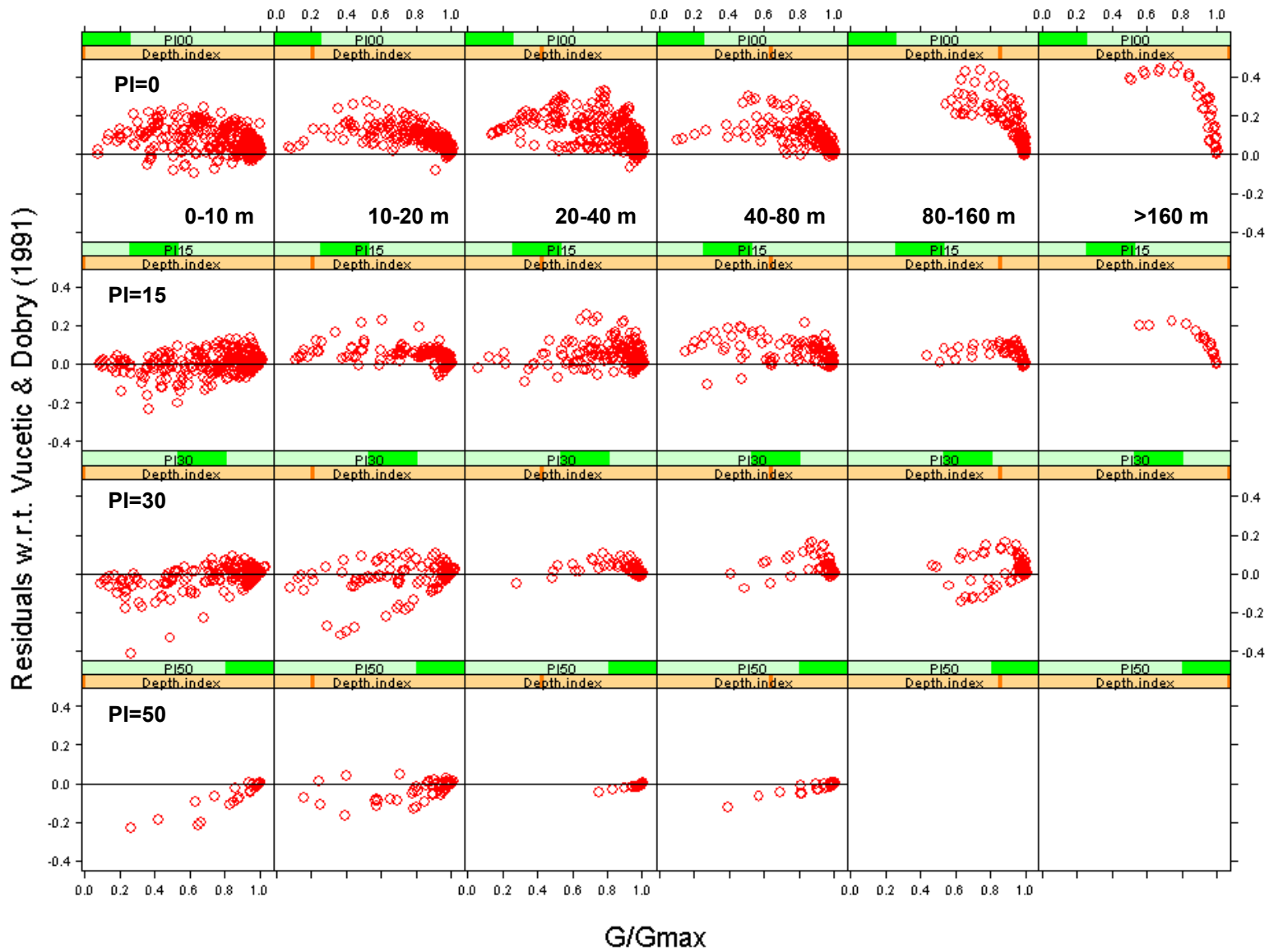
Figure 14a. Residuals in G/Gm laboratory observations and Vucetic & Dobry [4] model predictions.
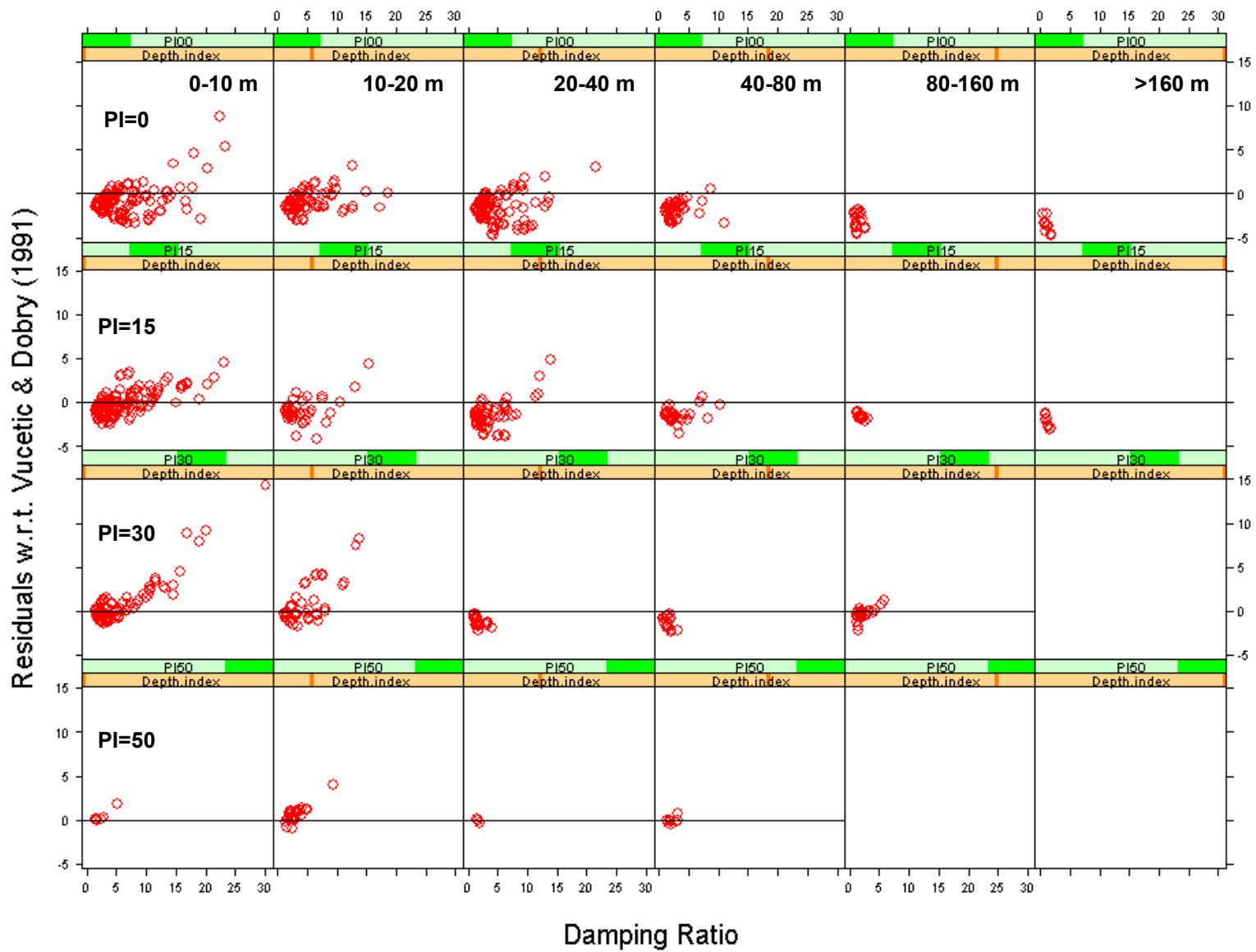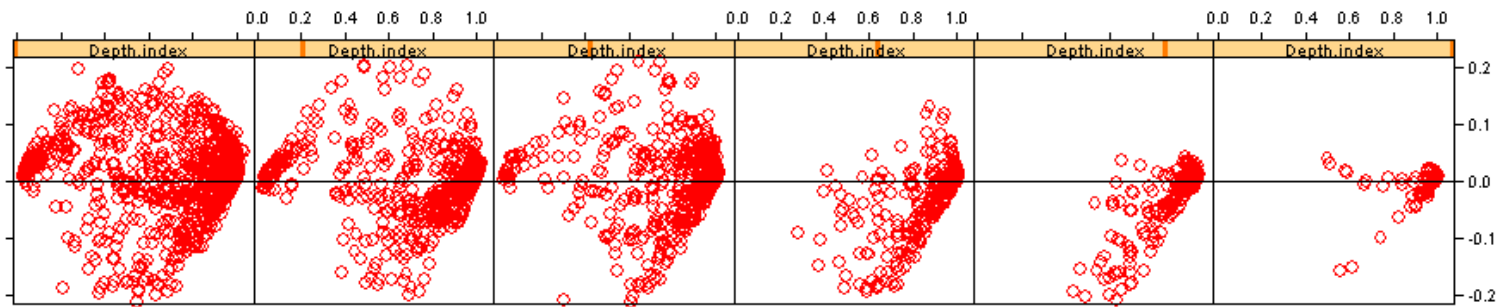
Figure 14b. Residuals in D between TS and DSDSS laboratory observations and Vucetic & Dobry [4] model predictions.

Normalized Modulus (G/Gm)

Damping (D)

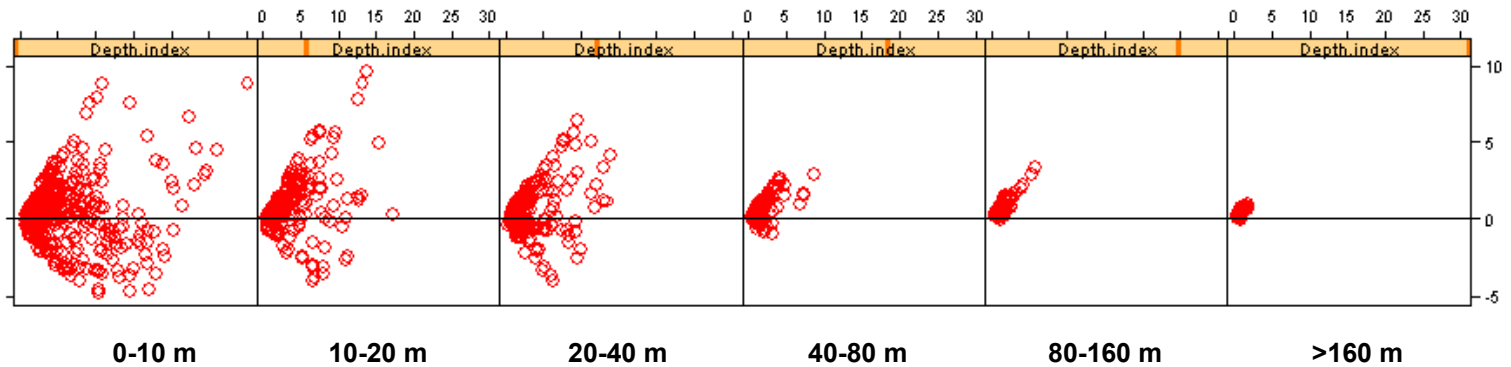| 0-10 m | 10-20 m | 20-40 m | 40-80 m | 80-160 m | >160 m |

Figure 15.   Residuals in G/Gm (top) and D (bottom) laboratory observations and Darendelli & Stokoe [1, 2] model predictions

ACKNOWLEDGMENTS

REFERENCES

[1] Darendelli, M.B., (2001), "A New Family of Normalized Modulus Reduction and Material Damping Curves", PhD Dissertation, University of Texas at Austin, 362 p.

[2] Darendeli, M.B., K.H. Stokoe, and R. Gilbert, (2002), "Development of a New Family of Normalized Modulus Reduction and Material Damping Curves", Presentation to March 2002 PEER-LL Quarterly Coordination Meeting, Pacific Earthquake Engineering Research Center.

[3] Seed, H.B., R.T. Wong, I.M. Idriss, and K. Tokimatsu, (1986), "Moduli and Damping Factors for Dynamic Analysis of Cohesionless Soils", Journal of the Soil Mechanics and Foundations Division, ASCE, Vol. 112, No. SM11, November, pp. 1016-1032.

[4] Vucetic, M. and R. Dobry, (1991), "Effects of Soil Plasticity on Cyclic Response", Journal of Geotechnical Engineering, Vol. 117, No. 1, January, pp. 89-107.

[5] Idriss, I.M. and J.I. Sun, (1992), "SHAKE91 – A Computer Program for Conducting Equivalent Linear Response Analysis of Horizontally Layered Soil Deposits", User Manual, University of California at Davis, November.

[6] Pyke, R. (1993), "Modeling of Dynamic Soil Properties", Appendix 7.A, Volume II, EPRI 1993 Report on Guidelines for Determining Design Basis Ground Motions, EPRI Early Site Demonstration Program, March.

[7] Stokoe, K.H., (1993), "Dynamic Properties of Undisturbed Soils from Treasure Island, California, Gilroy #2, California, and Lotung, Taiwan", Appendices 8.B1, 8.B2, and 8.B3, Volume IV, EPRI 1993 Report on Guidelines for Determining Design Basis Ground Motions, EPRI Early Site Demonstration Program, March.

[8] Silva, W.J., N. Abrahamson, G. Toro, and C. Costantino, (1997), "Description and Validation of the Stochastic Ground Motion Model", Report to Brookhaven National Laboratory, Associated Universities, Inc. Upton, NY.

[9] EPRI, (1993), "Early Site Permit Demonstration Program: Guidelines for Determining Design Basis Ground Motions – Volumes I thru IV", March.

[10] ROSRINE, (2000), ROSRINE: "Resolution of Site Response Issues from the Northridge Earthquake" [Online], Available: http://geoinfo.usc.edu/rosrine/.

[11] Nigbor, R.L., J.N. Swift, J.P. Bardet, J. Hu, (2001), "The ROSRINE Geotechnical Engineering Database and Website", Paper 1.3 in Proceedings of the COSMOS/PEER-LL Workshop on Archiving and Web Dissemination of Geotechnical Data, Consortium of Organizations for Strong-Motion Observation Systems, October 4-5, 2001.

[12] Doroudian, M. and M. Vucetic, (1995), "A Direct Simple Shear Device for Measuring Small-Strain Behavior", ASTM Geotechnical Testing Journal, Vol. 18, No. 1, pp.69-85.

[13] Darendelli, M.B., and K.H. Stokoe, (1997), "Dynamic Properties of Soils Subjected to the 1994 Northridge Earthquake", Geotechnical Engineering Report GR97-5, Civil Engineering Department, University of Texas at Austin, Austin, TX, December.

[14] Tabata, K., and M. Vucetic, (2000), "Results of Cyclic Simple Shear Tests on Thirteen Soils from Los Angeles Basin Conducted for ROSRINE Project and Other Research Purposes", UCLA Research Report No. ENG-00-219, November, 284 p.

[15] Anderson, D.G., (2003), "Laboratory Testing of Nonlinear Soil Properties: I & II", PEER-Lifelines Program Report, December.

[16] Tabata, K., and M. Vucetic, (2002), "Results of Cyclic Simple Shear Tests on Fifteen Soils Conducted for *PEARL* Project and Other Research Purposes", UCLA Research Report No. UCLA-Eng 02-233, November, 344 p.

[17] Stokoe, K.H., W.K. Choi, F-Y Menq, C. Valle, (2003), "Linear and Nonlinear Properties Determined by Combined Resonant Column and Torsional Shear Tests: Phase II of the ROSRINE Project, Volumes I and II", Geotechnical Engineering Report GR03-1, Geotechnical Engineering Center, University of Texas at Austin, March.

[18] NUPEC, (2000), "NUPEC Near Field Earthquake Project Site Investigations in California", Nuclear Power Engineering Corporation (NUPEC) Project Report submitted to the Ministry of International Trade and Industry (MITI) {In Japanese}.

[19] Stokoe, K.H., (2004), Personal communication re: lack of availability of electronic or tabulated text for the EPRI'93 data.

[20] Pyke, R. (1998), Personal communication re: concept of using field-to-lab modulus ratio as a disturbance adjustment factor on reference strain.

Table A1 – GeoIndex Model Values of Normalized Modulus and Damping Versus Strain

Depth Range [m]	Shear Strain [%]	1-PCA		2-FML		3-FMH	
		G/Gm	D	G/Gm	D	G/Gm	D
0-10	1.00E-04	0.993	1.34	0.997	1.32	0.999	1.32
	3.16E-04	0.981	1.43	0.991	1.37	0.996	1.35
	1.00E-03	0.950	1.71	0.974	1.53	0.987	1.45
	3.16E-03	0.877	2.53	0.931	2.02	0.962	1.78
	1.00E-02	0.729	4.64	0.827	3.38	0.891	2.75
	3.16E-02	0.503	8.65	0.630	6.56	0.725	5.30
	1.00E-01	0.275	13.39	0.376	11.67	0.460	10.42
	3.16E-01	0.125	16.97	0.176	16.72	0.216	17.00
	1.00E+00	0.051	18.80	0.071	19.86	0.082	21.95
	3.16E+00	0.020	19.04	0.026	20.83	0.028	23.84
10-20	1.00E-04	0.994	1.18	0.997	1.17	0.999	1.16
	3.16E-04	0.985	1.25	0.992	1.22	0.996	1.19
	1.00E-03	0.961	1.45	0.977	1.35	0.989	1.29
	3.16E-03	0.904	2.07	0.938	1.78	0.966	1.57
	1.00E-02	0.779	3.72	0.844	3.00	0.903	2.43
	3.16E-02	0.570	7.23	0.657	5.94	0.750	4.74
	1.00E-01	0.332	11.98	0.404	10.89	0.493	9.55
	3.16E-01	0.158	15.99	0.194	16.07	0.239	16.12
	1.00E+00	0.066	18.32	0.079	19.47	0.092	21.38
	3.16E+00	0.026	18.96	0.029	20.66	0.032	23.61
20-40	1.00E-04	0.996	1.04	0.997	1.04	0.999	1.03
	3.16E-04	0.989	1.09	0.993	1.08	0.997	1.06
	1.00E-03	0.971	1.24	0.980	1.20	0.990	1.14
	3.16E-03	0.925	1.69	0.945	1.58	0.970	1.39
	1.00E-02	0.823	2.96	0.858	2.67	0.914	2.15
	3.16E-02	0.636	5.90	0.682	5.36	0.774	4.22
	1.00E-01	0.396	10.50	0.433	10.15	0.526	8.73
	3.16E-01	0.198	14.88	0.213	15.42	0.264	15.23
	1.00E+00	0.085	17.71	0.088	19.07	0.104	20.79
	3.16E+00	0.034	18.80	0.033	20.49	0.036	23.37
40-80	1.00E-04	0.997	0.92	0.998	0.92	0.999	0.91
	3.16E-04	0.991	0.95	0.994	0.95	0.997	0.93
	1.00E-03	0.978	1.06	0.982	1.06	0.991	1.00
	3.16E-03	0.943	1.39	0.951	1.39	0.974	1.23
	1.00E-02	0.860	2.34	0.873	2.35	0.923	1.90
	3.16E-02	0.699	4.73	0.709	4.80	0.795	3.77
	1.00E-01	0.466	8.98	0.463	9.37	0.556	7.98
	3.16E-01	0.247	13.63	0.235	14.72	0.289	14.38
	1.00E+00	0.110	16.96	0.098	18.63	0.116	20.19
	3.16E+00	0.044	18.53	0.037	20.31	0.041	23.11
80-160	1.00E-04	0.998	0.81	0.998	0.81	0.999	0.81
	3.16E-04	0.994	0.83	0.996	0.83	0.997	0.83
	1.00E-03	0.984	0.90	0.988	0.90	0.992	0.90
	3.16E-03	0.959	1.12	0.966	1.12	0.974	1.12
	1.00E-02	0.898	1.78	0.910	1.78	0.925	1.77
	3.16E-02	0.769	3.53	0.781	3.56	0.800	3.59
	1.00E-01	0.556	7.14	0.559	7.37	0.564	7.73
	3.16E-01	0.320	11.91	0.310	12.72	0.295	14.09
	1.00E+00	0.150	15.83	0.138	17.34	0.119	19.96
	3.16E+00	0.062	18.05	0.054	19.84	0.042	22.97
>160	1.00E-04	0.998	0.71	0.999	0.71	0.999	0.71
	3.16E-04	0.996	0.72	0.997	0.72	0.998	0.72
	1.00E-03	0.989	0.77	0.992	0.77	0.994	0.77
	3.16E-03	0.971	0.91	0.977	0.91	0.983	0.91
	1.00E-02	0.927	1.35	0.937	1.35	0.950	1.34
	3.16E-02	0.827	2.58	0.840	2.60	0.859	2.60
	1.00E-01	0.643	5.46	0.651	5.58	0.664	5.76
	3.16E-01	0.404	10.03	0.398	10.58	0.390	11.48
	1.00E+00	0.203	14.45	0.190	15.73	0.171	17.93
	3.16E+00	0.087	17.33	0.077	19.07	0.063	22.12